Finite-Time Fuzzy Adaptive Constrained Tracking Control for Hypersonic Flight Vehicles with Singularity-Free Switching

Lv, Maolong; Li, Yongming; Pan, Wei; Baldi, Simone

DOI
10.1109/TMECH.2021.3090509

Publication date
2022

Document Version
Accepted author manuscript

Published in
IEEE/ASME Transactions on Mechatronics

Finite-Time Fuzzy Adaptive Constrained Tracking Control for Hypersonic Flight Vehicles with Singularity-Free Switching

Maolong Lv, Yongming Li, *Senior Member, IEEE,* Wei Pan, and Simone Baldi, *Senior Member, IEEE*

***Abstract*—This work proposes a fuzzy adaptive design solving the finite-time constrained tracking for hypersonic flight vehicles (HFVs). Actuator dynamics and asymmetric time-varying constraints are considered when solving this problem. The main features of the proposed design lie in: (a) introducing a novel piecewise but differentiable switching control law, with an appropriate design thought to avoid singularity issues typical of finite-time control; (b) handling actuator magnitude, bandwidth, and rate constraints, thanks to the introduction of an auxiliary compensating system counteracting the adverse effects caused by actuator physical constraints, while guaranteeing the closed-loop stability; (c) handling asymmetric time-varying state constraints, thanks to the introduction of tan-type barrier Lyapunov functions (BLFs) working for both constrained and unconstrained scenarios. Comparative simulation results illustrate the effectiveness of the proposed strategy over existing methods for HFVs in terms of convergence, smoothness, actuator performance, and constraints satisfaction.**

***Index Terms*—Hypersonic flight vehicle, finite-time stability, switching control, constrained tracking, singularity-free control.**

I. Introduction

Several studies on hypersonic flight vehicles (HFVs) have been carried out targeting future near-space transportation [1]-[6]. The design of guidance and control systems for HFVs presents a set of challenges, due to the complex interactions between the propulsion system, aerodynamics, and structural dynamics [7]-[9]. Research on flight control for HFVs in past decades can be primarily classified as sliding-mode control [10], PID control [11], dynamic inversion design [12] and intelligent control with radial basis function neural networks [13]-[14], fuzzy wavelet neural networks [7], or fuzzy logic systems [15]-[16]. Fuzzy logic systems (FLS) are particularly studied in HFVs, since the experience from expert human operators can be systematically included into fuzzy IF-THEN rules to be part of the control [16]. It should be mentioned that any practical control design for HFVs should not neglect crucial aspects of HFVs, such as finite-time tracking and constrained tracking (either state constraints or actuation constraints).

Recently, some HFVs literature [17]-[19] has highlighted the importance of *finite-time tracking* as compared to conventional non-finite-time tracking methods as in [1]-[16], due to its faster convergence rate. Finite-time tracking can be obtained via appropriate modifications to standard design methodologies. Most notably, the recursive backstepping method can be modified by introducing fractional feedback terms in virtual and actual control laws: the fractional terms guarantee convergence in finite time (see [20]-[23] and the references therein). However, those controllers cannot be safely utilized in HFVs due to the fact that singularity issue (non-differentiability) may occur in the derivatives of the fractional terms appearing in the control design (see Remark 2 and our case study in Sect. V.A for more details). Another standard design methodology, namely dynamic surface control (DSC), originally proposed in [24] to handle the issue of "explosion of complexity" in backstepping, is more challenging to be modified in finite-time tracking sense, due to the presence of linear filters that cannot ensure finite-time convergence of tracking errors.

With respect to state constrained tracking, it must be mentioned that HFVs utilize air-breathing supersonic combustion ramjet (scramjet) as the propulsion system to achieve sustained hypersonic flight [25]. To make the scramjet work perfectly, the flight path angle (FPA) and the pitch angle during hypersonic flight should be restricted inside some compact sets that are typically asymmetric and time-varying for ensuring efficiency of intake and combustion [26]. Although BLFs inspired by [27] have been proposed for HFVs to handle symmetric time-invariant constraints [28]-[30], these barriers cannot handle time-varying and possibly asymmetry operating regions of HFVs. Finally, with respect to actuation constraints (e.g. magnitude, bandwidth, and deflection rate) which arise naturally in HFVs deflectors and engines, we are not aware of any control design that can handle these phenomena in a rigorous (i.e. provably stable) way. To summarize, despite the progress in the field, several practically relevant problems are still open for HFVs. Motivated by above discussions, the main contributions of this paper are four-fold:

- Proposing a novel singularity-free approach to achieve fine-time tracking. To avoid the singularity issues, a piecewise but differentiable switching control law is introduced that

This work was supported by Double Innovation Plan under Grant 4207012004 and the Special Funding for Overseas talents under Grant 6207011901 (*Corresponding author: Simone Baldi*).

M. Lv is with the Delft Center for Systems and Control, Delft University of Technology, Mekelweg 2, Delft 2628 CD, The Netherlands (email: M.Lyu@tudelft.nl).

Y. Li is with the School of Science, Liaoning University of Technology, Jinzhou 121001, China (e-mail: liyongming1981@163.com).

W. Pan is with the Department of Cognitive Robotics, Delft University of Technology, 2628 CD Delft, The Netherlands (e-mail: wei.pan@tudelft.nl).

S. Baldi is with the School of Mathematics, Southeast University, Nanjing 210096, China, and also with the Delft Center for Systems and Control, Delft University of Technology, 2628 CD Delft, The Netherlands (e-mail: s.baldi@tudelft.nl).

guarantees the continuity and differentiability everywhere.

• Tan-type BLFs are appropriately embedded into the control design which are shown to handle asymmetric and time-varying flight state constraints. Interestingly, constrained trajectories not only ensure the boundedness of closed-loop signals but can also preserve the validity of fuzzy logic approximators.

• Actuator dynamics are modelled and tackled in terms of magnitude, bandwidth, and rate constraints, thanks to an auxiliary system constructed to generate certain compensating signals to counteract the adverse effects caused by actuator physical constraints.

• Finally, it is worth remarking that, in place of backstepping, a lower-complexity design is adopted in the framework of dynamic surface control [24]. The novelty of our design also lies in the use of both linear and fractional terms into the first-order filters, allowing the finite-time convergence properties.

The rest of this paper is structured as follows. Section II presents the problem formulation and preliminaries. The controller design for velocity subsystem and the altitude subsystem are given in Section III. Section IV proves the stability of the entire HFVs systems. In Section V, simulation results are given. Finally, Section VI concludes the work.

II. Problem Formulation and Preliminaries

A. Hypersonic Flight Vehicle Dynamics

The longitudinal dynamic model of HFVs under consideration was originally developed by Bolender and Doman [8], [31]-[32].

$$\dot{V} = \frac{T\cos\alpha - D}{m} - g\sin\gamma, \tag{1}$$

$$\dot{h} = V\sin\gamma, \tag{2}$$

$$\dot{\gamma} = \frac{L + T\sin\alpha}{mV} - \frac{g\cos\gamma}{V}, \tag{3}$$

$$\dot{\alpha} = Q - \frac{L + T\sin\alpha}{mV} + \frac{g\cos\gamma}{V}, \tag{4}$$

$$\dot{Q} = \frac{M}{I_{yy}}, \tag{5}$$

$$\ddot{\eta}_i = -2\zeta_i\omega_i\dot{\eta}_i - \omega_i^2\eta_i + N_i,\ i = 1,\ldots,n \tag{6}$$

where the lift L, drag D, pitching moment M, thrust T, generalized elastic forces N_i are given as

$$L \approx \bar{q}SC_L\left(\alpha,\delta_e,\delta_c,\boldsymbol{\eta}\right), \tag{7}$$

$$D \approx \bar{q}SC_D\left(\alpha,\delta_e,\delta_c,\boldsymbol{\eta}\right), \tag{8}$$

$$M \approx z_T T + \bar{q}S\bar{c}C_M\left(\alpha,\delta_e,\delta_c,\boldsymbol{\eta}\right), \tag{9}$$

$$T \approx \bar{q}S\left[C_{T,\Phi}\left(\alpha\right)\Phi + C_T\left(\alpha\right) + \boldsymbol{C}_T^{\boldsymbol{\eta}}\boldsymbol{\eta}\right], \tag{10}$$

$$N_i \approx \bar{q}S\big[N_i^{\alpha^2}\alpha^2 + N_i^{\alpha}\alpha + N_i^{\delta_e}\delta_e + N_i^{\delta_c}\delta_c + N_i^0 + \boldsymbol{N}_i^{\boldsymbol{\eta}}\boldsymbol{\eta}\big],\ i = 1,\ldots,n, \tag{11}$$

The model (1)-(11) contains five rigid-body states, i.e., velocity V, altitude h, FPA γ, angle of attack (AOA) α, and pitch rate Q, and three control inputs, i.e., the fuel equivalence ratio Φ, deflection of elevator δ_e, and deflection of canard δ_c. $\boldsymbol{\eta} = \left[\eta_1,\dot{\eta}_1,\ldots,\eta_n,\dot{\eta}_n\right]^{\mathrm{T}}$, $n \in \mathbb{N}^+$ are the flexible states with η_i being the amplitude of the ith bending mode. m, I_{yy}, g, ζ_i, ω_i, $\bar{q}$, S, z_T, and $\bar{c}$ represent the vehicle mass, moment of inertia, gravitational acceleration, damping ratio, flexible mode frequency, dynamic press, reference area, thrust moment arm, and reference length, respectively. The nonlinear functions in (7)-(11) are obtained from curve fitting as below

$$\begin{aligned}
C_M\left(\cdot\right) &= C_M^{\alpha^2}\alpha^2 + C_M^{\alpha}\alpha + C_M^{\delta_e}\delta_e + C_M^{\delta_c}\delta_c + C_M^0 + \boldsymbol{C}_M^{\boldsymbol{\eta}}\boldsymbol{\eta},\\
C_L\left(\cdot\right) &= C_L^{\alpha}\alpha + C_L^{\delta_e}\delta_e + C_L^{\delta_c}\delta_c + C_L^0 + \boldsymbol{C}_L^{\boldsymbol{\eta}}\boldsymbol{\eta},\\
C_D\left(\cdot\right) &= C_D^{\alpha^2}\alpha^2 + C_D^{\alpha}\alpha + C_D^{\delta_e^2}\delta_e^2 + C_D^{\delta_e}\delta_e\\
&\quad + C_D^{\delta_c^2}\delta_c^2 + C_D^{\delta_c}\delta_c + C_D^0 + \boldsymbol{C}_D^{\boldsymbol{\eta}}\boldsymbol{\eta},\\
C_{T,\Phi}\left(\cdot\right) &= C_{T,\Phi}^{\alpha^3}\alpha^3 + C_{T,\Phi}^{\alpha^2}\alpha^2 + C_{T,\Phi}^{\alpha}\alpha + C_{T,\Phi}^0,\\
C_T\left(\cdot\right) &= C_T^{\alpha^3}\alpha^3 + C_T^{\alpha^2}\alpha^2 + C_T^{\alpha}\alpha + C_T^0,\\
\boldsymbol{C}_j^{\boldsymbol{\eta}} &= \left[C_j^{\eta_1},0,\ldots,C_j^{\eta_n},0\right],\ j = T,M,L,D,\\
\boldsymbol{N}_i^{\boldsymbol{\eta}} &= \left[N_i^{\eta_1},0,\ldots,N_i^{\eta_n},0\right],\ i = 1,\ldots,n.
\end{aligned} \tag{12}$$

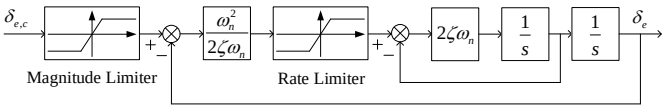

Fig. 1: Filter that generates magnitude, bandwidth, and rate constraints.

To cancel the lift-elevator coupling, δ_c is set to be ganged with δ_e, i.e., $\delta_c = k_{e,c}\delta_e$ with $k_{e,c} = -C_L^{\delta_e}/C_L^{\delta_c}$. Thereby, the control inputs of HFVs become Φ and δ_e. This approach was originally proposed in [25] as a way to remove some non-minimum phase characteristics of the dynamics. The deflection of the elevator δ_e is adjusted through an electric actuator which can be well approximated by the following second-order dynamics:

$$\ddot{\delta}_e = -2\zeta\omega_n\dot{\delta}_e - \omega_n^2\delta_e + \omega_n^2\delta_{e,c} \tag{13}$$

where ω_n is the undamped natural frequency and ζ is the damping ratio. Dynamics (13) can capture magnitude, bandwidth, and rate constraints, if the input signal δ_e is eventually obtained by the command $\delta_{e,c}$ filtered through a linear, stable, low-pass command filter as shown in Fig. 1. Similarly, the input signal Φ can be obtained by the command Φ_c filtered in a similar way as Fig. 1.

The control objective of this paper is to design the control inputs Φ_c and $\delta_{e,c}$ for system (1)-(6) and (13) such that the variables V and h follow the reference commands V_{ref} and h_{ref} with finite-time guarantees, while flight state variables are confined within asymmetric and time-varying compact sets all the time.

The elevator angular deflection δ_e primarily affects the AOA α (hence altitude h), whereas the fuel equivalence ratio Φ primarily affects the thrust T (hence velocity V). Based on these physical considerations, related literature has proposed a model decomposition amenable for control design [12]-[13].

B. Model Decomposition and State Constraints

The decomposition relies on separating the motion model of HFVs into the velocity and altitude subsystems. Taking

aerodynamic parameter uncertainties and external disturbances into account, the velocity subsystem can be rewritten as

$$\dot{V} = \boldsymbol{\zeta}_V^{\mathrm{T}}(\boldsymbol{f}_V + \boldsymbol{g}_V\Phi) + d_V, \tag{14}$$

where $\boldsymbol{\zeta}_V = \frac{S}{m}\big[C_{T,\Phi}^{\alpha^3}, C_{T,\Phi}^{\alpha^2}, C_{T,\Phi}^{\alpha}, C_{T,\Phi}^{0}, C_{T}^{\alpha^3}, C_{T}^{\alpha^2}, C_{T}^{\alpha}, C_{T}^{0}, C_{D}^{\alpha^2}, C_{D}^{\alpha}, (C_{D}^{\delta_e^2} + k_{e,c}^2 C_{D}^{\delta_c^2}), (C_{D}^{\delta_e} + k_{e,c} C_{D}^{\delta_c}), C_{D}^{0}, \frac{m}{S}\big]^{\mathrm{T}}$, $\boldsymbol{g}_V = \bar{q}\cos\alpha\big[\alpha^3, \alpha^2, \alpha, 1, \boldsymbol{0}^{1\times 10}\big]^{\mathrm{T}}$, $\boldsymbol{f}_V = \bar{q}\big[\boldsymbol{0}^{1\times 4}, \alpha^3\cos\alpha, \alpha^2\cos\alpha, \alpha\cos\alpha, \cos\alpha, -\alpha^2, -\alpha, -\delta_e^2, -\delta_e, -1, -\frac{g}{\bar{q}}\sin\gamma\big]^{\mathrm{T}}$, and the lumped disturbance $d_V = \frac{\bar{q}S}{m}\boldsymbol{C}_T^{\boldsymbol{\eta}}\boldsymbol{\eta}\cos\alpha - \frac{\bar{q}S}{m}\boldsymbol{C}_D^{\boldsymbol{\eta}}\boldsymbol{\eta} + \Delta_V$ with Δ_V denoting the perturbations resulting from coefficients uncertainties and external disturbances in the velocity subsystem.

As the FPA γ and AOA α are quite small during the cruise phase, the literature has proposed to take $\sin\gamma \approx \gamma$ in (2) and neglect $T\sin\alpha$ in (3) for simplicity [12]-[13]. Therefore, the altitude subsystem can be rewritten as

$$\begin{cases} \dot{h} = V\gamma, \\ \dot{\gamma} = \boldsymbol{\zeta}_\gamma^{\mathrm{T}}(\boldsymbol{f}_\gamma + \boldsymbol{g}_\gamma\alpha) + d_\gamma, \\ \dot{\alpha} = \boldsymbol{\zeta}_\alpha^{\mathrm{T}}(\boldsymbol{f}_\alpha + \boldsymbol{g}_\alpha Q) + d_\alpha, \\ \dot{Q} = \boldsymbol{\zeta}_Q^{\mathrm{T}}(\boldsymbol{f}_Q + \boldsymbol{g}_Q\delta_e) + d_Q, \end{cases} \tag{15}$$

where $\boldsymbol{\zeta}_\gamma = \big[\frac{S}{m}C_L^{\alpha}, \frac{S}{m}C_L^{0}, 1\big]^{\mathrm{T}}$, $\boldsymbol{\zeta}_\alpha = \big[1, \frac{S}{m}C_L^{\alpha}, \frac{S}{m}C_L^{0}, 1\big]^{\mathrm{T}}$, $\boldsymbol{\zeta}_Q = \frac{S}{I_{yy}}\big[\bar{c}C_M^{\delta_e}, \bar{c}k_{e,c}C_M^{\delta_c}, z_T C_{T,\Phi}^{\alpha^3}, z_T C_{T,\Phi}^{\alpha^2}, z_T C_{T,\Phi}^{\alpha}, z_T C_{T,\Phi}^{0}, z_T C_T^{\alpha^3}, (z_T C_T^{\alpha^2} + \bar{c}C_M^{\alpha^2}), (z_T C_T^{\alpha} + \bar{c}C_M^{\alpha}), (z_T C_T^{0} + \bar{c}C_M^{0})\big]^{\mathrm{T}}$, $\boldsymbol{g}_\gamma = \big[\frac{\bar{q}}{V}, \boldsymbol{0}^{1\times 2}\big]^{\mathrm{T}}$, $\boldsymbol{g}_\alpha = \big[1, \boldsymbol{0}^{1\times 3}\big]^{\mathrm{T}}$, $\boldsymbol{g}_Q = \big[\bar{q}, \bar{q}, \boldsymbol{0}^{1\times 8}\big]^{\mathrm{T}}$, $\boldsymbol{f}_\gamma = \big[0, \frac{\bar{q}}{V}, -\frac{g}{V}\cos\gamma\big]^{\mathrm{T}}$, $\boldsymbol{f}_\alpha = \frac{\bar{q}}{V}\big[0, -\alpha, -1, \frac{g}{\bar{q}}\cos\gamma\big]^{\mathrm{T}}$, $\boldsymbol{f}_Q = \bar{q}\big[\boldsymbol{0}^{1\times 2}, \alpha^3\Phi, \alpha^2\Phi, \alpha\Phi, \Phi, \alpha^3, \alpha^2, \alpha, 1\big]^{\mathrm{T}}$, and the lumped disturbances $d_\gamma = \frac{\bar{q}S}{mV}\boldsymbol{C}_L^{\boldsymbol{\eta}}\boldsymbol{\eta} + \Delta_\gamma$, $d_\alpha = -\frac{\bar{q}S}{mV}\boldsymbol{C}_L^{\boldsymbol{\eta}}\boldsymbol{\eta} + \Delta_\alpha$, and $d_Q = \frac{z_T\bar{q}S}{I_{yy}}\boldsymbol{C}_T^{\boldsymbol{\eta}}\boldsymbol{\eta} + \frac{\bar{q}S\bar{c}}{I_{yy}}\boldsymbol{C}_M^{\boldsymbol{\eta}}\boldsymbol{\eta} + \Delta_Q$, with Δ_γ, Δ_α, and Δ_Q representing the perturbations resulting from coefficient uncertainties and external disturbances in the altitude subsystem.

C. Technical Key Lemmas

The following results, which are often adopted in control of nonlinear systems, will be used for stability analysis.

Assumption 1 [33]: The reference commands V_{ref}, $\dot{V}_{ref}$, $\ddot{V}_{ref}$, h_{ref}, $\dot{h}_{ref}$, and $\ddot{h}_{ref}$ are in a bounded region Ω_{ref}. In fact, in flight control it is common for HFVs to track velocities and altitudes whose first and second derivative are bounded.

Lemma 1 [34]: For any constants $m > 0, x \geq 0, y > 0$, the inequality $x^m(y-x) \leq \frac{1}{1+m}\left(y^{1+m} - x^{1+m}\right)$ always holds.

Lemma 2 [35]: The inequality $(\iota - \vartheta)^r \geq \vartheta^r - \iota^r$ holds for $\vartheta \leq \iota, r > 1, \iota > 0$.

Lemma 3 [36]: Consider the Lyapunov characterization of finite-time stability in the form $\dot{L}(x) \leq -\varsigma_1 L(x) - \varsigma_2 L^l(x)$, where $\varsigma_1 > 0$, $\varsigma_2 > 0$, and $0 < l < 1$ are scalars. Then, $L(x)$ is convergent to a residual set with a finite time $T_0 \leq \varsigma_1^{-1}(1-l)^{-1}\ln\big[\big(\varsigma_1 L^{1-l}(x_0) + \varsigma_2\big)\varsigma_2^{-1}\big]$.

Lemma 4 [37]: The inequality $\Big(\sum_{i=1}^{n}|x_i|\Big)^l \leq \sum_{i=1}^{n}|x_i|^l \leq n^{1-l}\Big(\sum_{i=1}^{n}|x_i|\Big)^l$ holds for $x_i \in \mathbb{R}$, $i = 1, \ldots, n$, $0 < l \leq 1$.

Lemma 5 [38]: Let a function $\kappa(t) \in \mathbb{R}$ satisfy

$$\dot{\kappa}(t) + \lambda_0\kappa(t) - \ell(t) + \lambda_1\kappa^{\frac{l_1}{l_2}}(t) = 0, \tag{16}$$

where l_1 and l_2 are positive odd integers satisfying $0 \leq \frac{l_1}{l_2} < 1$, λ_0 and λ_1 are positive constants, and $\ell(t)$ is a positive function. Then, it holds that $\kappa(t) \geq 0$ for $\forall t \geq 0$ as long as $\kappa(0) \geq 0$.

FLSs are used to approximate system continuous unknown dynamics thanks to the following result.

Lemma 6 [39]-[41]: Define a set of fuzzy IF-THEN rules, where the lth IF-THEN rule is written as

$$\mathcal{R}^l: \text{If } x_1 \text{ is } F_1^l, \text{ and } \ldots \text{ and } x_n \text{ is } F_n^l, \text{ then } y \text{ is } B^l.$$

where $\boldsymbol{x} = [x_1, \ldots, x_n]^{\mathrm{T}} \in \mathbb{R}^n$, and $y \in \mathbb{R}$ are the input and output of the fuzzy logic systems, $F_1^l, \ldots, F_n^l$ and B^l are fuzzy sets in $\mathbb{R}$. Let $F(\boldsymbol{x})$ be a continuous function defined on a compact set $\Omega_{\boldsymbol{x}}$. Then, for a given desired level of accuracy $\varepsilon' > 0$, there exists a fuzzy logic system $\boldsymbol{W}^{\mathrm{T}}\boldsymbol{\varphi}(\boldsymbol{x})$ such that

$$\sup_{\boldsymbol{x}\in\Omega_{\boldsymbol{x}}}|F(\boldsymbol{x}) - \boldsymbol{W}^{\mathrm{T}}\boldsymbol{\varphi}(\boldsymbol{x})| \leq \varepsilon', \tag{17}$$

where $\boldsymbol{W} = [w_1, \ldots, w_p]^{\mathrm{T}}$ is the adaptive fuzzy parameter vector in a compact set $\Omega_{\boldsymbol{W}}$, p is the number of the fuzzy rules, $\boldsymbol{\varphi}(\boldsymbol{x}) = [\phi_1(\boldsymbol{x}), \ldots, \phi_p(\boldsymbol{x})]^{\mathrm{T}}$ is the fuzzy basis function vector, and $\phi_l(\boldsymbol{x}) = \prod_{j=1}^{p}\mu_{F_j^l}(x_j)\big/\sum_{l=1}^{p}(\prod_{j=1}^{m}\mu_{F_j^l}(x_j))$ with $\mu_{F_j^l}(x_j)$ being a fuzzy membership function of the variable x_j in IF-THEN rule. Let $\boldsymbol{W}^*$ be the optimal parameter vector, which is defined as

$$\boldsymbol{W}^* = \arg\min_{\boldsymbol{W}\in\Omega_{\boldsymbol{W}}}\left\{\sup_{\boldsymbol{x}\in\Omega_{\boldsymbol{x}}}|F(\boldsymbol{x}) - \boldsymbol{W}^{\mathrm{T}}\boldsymbol{\varphi}(\boldsymbol{x})|\right\}. \tag{18}$$

Then, we can obtain

$$F(\boldsymbol{x}) = \boldsymbol{W}^{*\mathrm{T}}\boldsymbol{\varphi}(\boldsymbol{x}) + \varepsilon, \tag{19}$$

where ε is the minimum fuzzy approximation error.

III. Finite-Time Fuzzy Adaptive Control Design

In view of the decomposition of Sect. II.B, the control design is also decomposed in a velocity control design and an altitude control design (also refer to Fig. 2). It is worth mentioning that, due to asymmetric constraints, both designs rely on skillfully constructing asymmetric time-varying BLFs, in which the upper and lower thresholds $k_{b_\star}(t)$ and $k_{a_\star}(t)$ can be set independently.

A. Velocity Control Design

Define the tracking error $z_V = \tilde{V} - e_V$, where $\tilde{V} = V - V_{ref}$ and e_V is an auxiliary variable which will be defined later. On this basis, construct the asymmetric time-varying BLF as follows

$$L_V = \frac{k_V^2(z_V(t))}{\pi}\tan\left(\frac{\pi z_V^2(t)}{2k_V^2(z_V(t))}\right), \tag{20}$$

where $k_\star(z_\star(t))$ is a short notation for the asymmetric time-varying threshold, i.e.

$$k_\star(z_\star(t)) \triangleq \begin{cases} k_{b_\star}(t), & \text{if } z_\star(t) > 0, \\ k_{a_\star}(t), & \text{if } z_\star(t) \leq 0. \end{cases} \tag{21}$$

Throughout this paper, we abbreviate $k_\star(z_\star(t))$ by $k_\star(t)$ for notation simplicity. To highlight the time-varying mature

This article has been accepted for publication in a future issue of this journal, but has not been fully edited. Content may change prior to final publication. Citation information: DOI 10.1109/TMECH.2021.3090509, IEEE/ASME Transactions on Mechatronics

of the state constraints, the time variable t is not omitted in $k_\star(t)$, whereas it can be omitted for other variables.

Remark 1: The tan-type BLF (20) is asymmetric, time-varying, and positive definite. Besides, according to L'Hopital's rule, we have $\lim_{k_V(t)\to\infty} L_V = \frac{1}{2}z_V^2$, implying that both constrained and unconstrained cases can be encompassed by (20). Note that conventional BLFs (e.g. log-type BLFs) cannot deal with the unconstrained condition since $\lim_{k_V(t)\to\infty} \frac{1}{2}\log\left(\frac{k_V^2(t)}{k_V^2(t)-z_V^2}\right) = 0$.

It follows from (14) and (20) that the time derivative of L_V is

$$\dot{L}_V = \hbar_V\left(\boldsymbol{\zeta}_V^{\mathrm{T}}\boldsymbol{g}_V\Phi + F_V(\boldsymbol{x}_V) - \frac{\dot{k}_V(t)}{k_V(t)}z_V\right) + \frac{2k_V(t)\dot{k}_V(t)}{\pi}\tan\left(\frac{\pi z_V^2}{2k_V^2(t)}\right), \quad (22)$$

where $\hbar_V = \frac{z_V}{\cos^2\left(\frac{\pi z_V^2}{2k_V^2(t)}\right)}$. $F_V(\boldsymbol{x}_V) = \boldsymbol{\zeta}_V^{\mathrm{T}}\boldsymbol{f}_V + d_V - \dot{V}_{ref}$ collects the unknown dynamics with $\boldsymbol{x}_V = V$. According to Lemma 6, $F_V(\boldsymbol{x}_V)$ can be approximated by an FLS as $F_V(\boldsymbol{x}_V) = \boldsymbol{W}_V^{*\mathrm{T}}\boldsymbol{\varphi}_V(\boldsymbol{x}_V) + \varepsilon_V$ over a compact set Ω_V, where ε_V is such that $|\varepsilon_V| \le \varepsilon_V^*$ with $\varepsilon_V^* > 0$ a constant.

The control law Φ_c is constructed as

$$\Phi_c = -\frac{1}{\boldsymbol{\zeta}_V^{\mathrm{T}}\boldsymbol{g}_V}\left[\frac{c_V}{\hbar_V}\tan\left(\frac{\pi z_V^2}{2k_V^2(t)}\right) + \frac{\mu_V}{\hbar_V}S_{V1} + \frac{1}{2}(p+2)\frac{S_{V2}}{\hbar_V} + \frac{1}{2}\hbar_V\hat{\Xi}_V + M_V\tilde{V} + \frac{2k_V(t)\dot{k}_V(t)}{\pi\hbar_V}\tan\left(\frac{\pi z_V^2}{2k_V^2(t)}\right)\right], \quad (23)$$

where $0 < l < 1$, p is the number of the fuzzy rules, $\mu_V > 0$ and $c_V > 0$ are design parameters, $\hat{\Xi}_V$ is the estimate of $\Xi_V = ||\boldsymbol{W}_V^*||^2$, and the switching terms S_{V1} and S_{V2} are designed as follows

$$S_{V1} = \begin{cases} \tan^l\left(\frac{\pi z_V^2}{2k_V^2(t)}\right), & \text{if } |z_V| \ge \tau_V, \\ \tan^{l-1}\left(\frac{\pi\tau_V^2}{2k_V^2(t)}\right)\tan\left(\frac{\pi z_V^2}{2k_V^2(t)}\right), & \text{otherwise}, \end{cases} \quad (24)$$

$$S_{V2} = \begin{cases} 1, & \text{if } |z_V| \ge \tau_V, \\ \tan^{-1}\left(\frac{\pi\tau_V^2}{2k_V^2(t)}\right)\tan\left(\frac{\pi z_V^2}{2k_V^2(t)}\right), & \text{otherwise}. \end{cases} \quad (25)$$

The time-varying gain term M_V in (23) is given by

$$M_V = \sqrt{\left(\frac{\dot{k}_{aV}}{k_{aV}}\right)^2 + \left(\frac{\dot{k}_{bV}}{k_{bV}}\right)^2 + o_V}, \quad (26)$$

where $o_V > 0$ is a parameter to be designed.

As a next step, we design the following auxiliary system to handle the constraints imposed on control signal Φ_c

$$\dot{e}_V = -M_V e_V + \boldsymbol{\zeta}_V^{\mathrm{T}}\boldsymbol{g}_V(\Phi - \Phi_c), \quad (27)$$

The adaptation law $\dot{\hat{\Xi}}_V$ is designed as

$$\dot{\hat{\Xi}}_V = \frac{1}{2}\hbar_V^2\rho_V - \rho_V\hat{\Xi}_V - \rho_V\hat{\Xi}_V^l, \quad (28)$$

where ρ_V is a positive design constant. By applying Lemma 5, we know that $\hat{\Xi}_V(t) \ge 0$ for $\forall t > 0$ after choosing $\hat{\Xi}_V(0) \ge 0$. Consider the Lyapunov function candidate $\bar{L}_V = L_V + \frac{1}{2\rho_V}\tilde{\Xi}_V^2$ with $\tilde{\Xi}_V = \Xi_V - \hat{\Xi}_V$, the time derivative of $\bar{L}_V$ can be expressed as

$$\dot{\bar{L}}_V = \dot{L}_V - \frac{1}{\rho_V}\tilde{\Xi}_V\dot{\hat{\Xi}}_V. \quad (29)$$

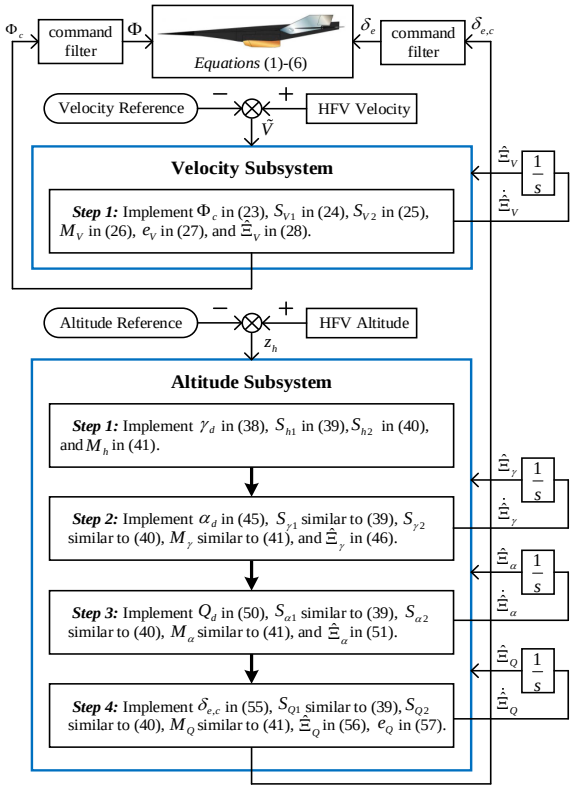

Fig. 2: The framework of the proposed control structure.

Substituting (23) and (28) into (29) yields

$$\dot{\bar{L}}_V \le -c_V\tan\left(\frac{\pi z_V^2}{2k_V^2(t)}\right) - \mu_V S_{V1} - \frac{1}{2}(p+2)S_{V2} + \hbar_V F_V(\boldsymbol{x}_V) - M_V\hbar_V z_V - \frac{\dot{k}_V(t)}{k_V(t)}\hbar_V z_V - \frac{1}{2}\hbar_V^2\Xi_V + \tilde{\Xi}_V\hat{\Xi}_V + \tilde{\Xi}_V\hat{\Xi}_V^l, \quad (30)$$

where

$$-M_V\hbar_V z_V - \frac{\dot{k}_V(t)}{k_V(t)}\hbar_V z_V = \left(-M_V - \frac{\dot{k}_V(t)}{k_V(t)}\right)\frac{z_V^2}{\cos^2\left(\frac{\pi z_V^2}{2k_V^2(t)}\right)} < 0. \quad (31)$$

Let $\bar{\boldsymbol{W}}_V = [\boldsymbol{W}_V^*, \varepsilon_V, S_{V1}]^{\mathrm{T}}$, $\bar{\boldsymbol{\varphi}}_V = [\boldsymbol{\varphi}_V(\boldsymbol{x}_V), 1, 1]^{\mathrm{T}}$, one has

$$\hbar_V F_V(\boldsymbol{x}_V) \le \hbar_V\left\|\bar{\boldsymbol{W}}_V\right\|\left\|\bar{\boldsymbol{\varphi}}_V\right\| \le \frac{1}{2}\left(p + 2 + \hbar_V^2\Xi_V\right). \quad (32)$$

Substituting (31) and (32) into (30) leads to

$$\dot{\tilde{L}}_V \leq -c_V \tan\left(\frac{\pi z_V^2}{2k_V^2(t)}\right) - \mu_V S_{V1} - \frac{1}{2}(p+2)(S_{V2}-1) + \tilde{\Xi}_V \hat{\Xi}_V + \tilde{\Xi}_V \hat{\Xi}_V^l, \tag{33}$$

which will be later used for stability analysis.

B. Altitude Control Design

Step 1: Define the tracking error as $z_h = h - h_{ref}$, and construct the asymmetric time-varying BLF as

$$L_h = \frac{k_h^2(z_h(t))}{\pi} \tan\left(\frac{\pi z_h^2(t)}{2k_h^2(z_h(t))}\right). \tag{34}$$

Taking the derivative of L_h yields

$$\dot{L}_h = \hbar_h \left(V\gamma - \dot{h}_{ref} - \frac{\dot{k}_h(t)}{k_h(t)} z_h\right) + \frac{2k_h(t)\dot{k}_h(t)}{\pi} \tan\left(\frac{\pi z_h^2}{2k_h^2(t)}\right), \tag{35}$$

where $\hbar_h = \frac{z_h}{\cos^2\left(\frac{\pi z_h^2}{2k_h^2(t)}\right)}$.

To proceed with the finite-time control design, we propose a dynamic surface control method appropriately modified to the purpose of differentiability. Firstly, let us consider the coordinate transformation [42]

$$\begin{cases} z_\gamma = \gamma - \gamma_c, & z_\alpha = \alpha - \alpha_c, & z_Q = \tilde{Q} - e_Q, \\ y_\gamma = \gamma_c - \gamma_d, & y_\alpha = \alpha_c - \alpha_d, & y_Q = Q_c - Q_d, \end{cases} \tag{36}$$

where z_γ, z_α, z_Q are the tracking errors, $\tilde{Q} = Q - Q_d$, e_Q is an auxiliary variable defined later, γ_d, α_d and Q_d are the virtual control laws, y_γ, y_α, y_Q are the boundary layer errors, γ_c, α_c and Q_c are the outputs of first-order filters defined by

$$\begin{cases} \dot{\gamma}_c = -\tau_{\gamma 1} y_\gamma - \tau_{\gamma 2} y_\gamma^l, \\ \dot{\alpha}_c = -\tau_{\alpha 1} y_\alpha - \tau_{\alpha 2} y_\alpha^l, \\ \dot{Q}_c = -\tau_{Q1} y_Q - \tau_{Q2} y_Q^l, \end{cases} \tag{37}$$

where $\tau_{\gamma 1}$, $\tau_{\gamma 2}$, $\tau_{\alpha 1}$, $\tau_{\alpha 2}$, τ_{Q1}, and τ_{Q2} are the positive design constants, and $0 < l = l_1/l_2 < 1$ with l_1, l_2 being positive odd integers.

Construct the virtual control law γ_d as

$$\gamma_d = -\frac{1}{V}\left[\frac{c_h}{\hbar_h}\tan\left(\frac{\pi z_h^2}{2k_h^2(t)}\right) + \frac{\mu_h}{\hbar_h} S_{h1} + \frac{1}{2}(p+2)\frac{S_{h2}}{\hbar_h} - \dot{h}_{ref} + M_h z_h + \frac{2k_h(t)\dot{k}_h(t)}{\pi\hbar_h}\tan\left(\frac{\pi z_h^2}{2k_h^2(t)}\right)\right], \tag{38}$$

where μ_h and c_h are the positive design parameters, the switching term $S_{\gamma 1}$ and $S_{\gamma 2}$ are designed as follows

$$S_{h1} = \begin{cases} \tan^l\left(\frac{\pi z_h^2}{2k_h^2(t)}\right), & \text{if } |z_h| \geq \tau_h, \\ \tan^{l-1}\left(\frac{\pi \tau_h^2}{2k_h^2(t)}\right)\tan\left(\frac{\pi z_h^2}{2k_h^2(t)}\right), & \text{otherwise}, \end{cases} \tag{39}$$

$$S_{h2} = \begin{cases} 1, & \text{if } |z_h| \geq \tau_h, \\ \tan^{-1}\left(\frac{\pi \tau_h^2}{2k_h^2(t)}\right)\tan\left(\frac{\pi z_h^2}{2k_h^2(t)}\right), & \text{otherwise}. \end{cases} \tag{40}$$

Remark 2: One novelty in (39) and (40) is represented by the switching functions S_{h1} and S_{h2}. In fact, in order to achieve finite-time tracking, conventional designs use the fractional powers of tracking error z_h^l with $0 < l < 1$ for $\forall z_h \in \mathbb{R}$ (cf. [20, eq.(7)], [21, eq.(22)], [22, eq.(29)], [23, eq.(42)], etc). However, because $\dot{z}_h^l = l z_h^{l-1} \to \infty$ as $z_h \to 0$, a singularity problem (cf. our case study in Sect. V.A) will arise in the virtual control law. A similar problem arises also in designs that are alternative to backstepping, such as terminal sliding mode (cf. the fractional powers in [17, eq. (46) and eq. (51)] whose derivative must be calculated for control design). On the contrary, the switching functions (39) and (40) are skillfully designed to remove this singularity. Continuity of S_{h1}, $\dot{S}_{h1}$, S_{h2} and $\dot{S}_{h2}$ holds due to the following facts:

$$\begin{aligned} \lim_{z_h \to \tau_h^-} S_{h1} &= \lim_{z_h \to \tau_h^+} S_{h1} = \tan^l\left(\frac{\pi \tau_h^2}{2k_h^2(t)}\right), \\ \lim_{z_h \to \tau_h^-} \dot{S}_{h1} &= \lim_{z_h \to \tau_h^+} \dot{S}_{h1} \\ &= -\frac{\dot{k}_h(t)}{k_h^3(t)} \cdot \frac{\pi l \tau_h^2}{\cos^2\left(\frac{\pi \tau_h^2}{2k_h^2(t)}\right)} \tan^l\left(\frac{\pi \tau_h^2}{2k_h^2(t)}\right), \\ \lim_{z_h \to 0^-} S_{h1} &= \lim_{z_h \to 0^+} S_{h1} = 0, \ \lim_{z_h \to 0^-} \dot{S}_{h1} = \lim_{z_h \to 0^+} \dot{S}_{h1} = 0, \\ \lim_{z_h \to \tau_h^-} S_{h2} &= \lim_{z_h \to \tau_h^+} S_{h2} = 1, \ \lim_{z_h \to \tau_h^-} \dot{S}_{h2} = \lim_{z_h \to \tau_h^+} \dot{S}_{h2} = 0, \\ \lim_{z_h \to 0^-} S_{h2} &= \lim_{z_h \to 0^+} S_{h2} = 0, \ \lim_{z_h \to 0^-} \dot{S}_{h2} = \lim_{z_h \to 0^+} \dot{S}_{h2} = 0. \end{aligned}$$

The time-varying gain term M_h in (38) is designed as follows

$$M_h = \sqrt{\left(\frac{\dot{k}_{a_h}}{k_{a_h}}\right)^2 + \left(\frac{\dot{k}_{b_h}}{k_{b_h}}\right)^2 + o_h}, \tag{41}$$

in which $o_h > 0$ is the parameter to be designed. Substituting (38)-(41) into (35) and using $\gamma = z_\gamma + y_\gamma + \gamma_d$, the time derivative of L_h can be rewritten as

$$\dot{L}_h \leq V(z_\gamma + y_\gamma) - c_h \tan\left(\frac{\pi z_h^2}{2k_h^2(t)}\right) - \mu_h S_{h1} - \frac{1}{2}(p+2)(S_{h2}-1). \tag{42}$$

From (38) it can be deduced that γ_d and $\dot{\gamma}_d$ are functions of z_h, $\dot{z}_h$, $k_h(t)$, $\dot{k}_h(t)$, $\ddot{k}_h(t)$, $\dot{h}_{ref}$ and $\ddot{h}_{ref}$, respectively. Thanks to the continuity and differentiability of S_{h1} and S_{h2}, both functions γ_d and $\dot{\gamma}_d$ are continuous. Therefore, in accordance with (36) and (37), we get $\dot{y}_\gamma = -\tau_{\gamma 1} y_\gamma - \tau_{\gamma 2} y_\gamma^l + \iota_\gamma(z_h, \dot{z}_h, k_h(t), \dot{k}_h(t), \ddot{k}_h(t), \dot{h}_{ref}, \ddot{h}_{ref})$ with $\iota_\gamma(\cdot)$ being a continuous function.

Step 2: Construct the asymmetric time-varying BLF as

$$L_\gamma = L_h + \frac{k_\gamma^2(z_\gamma(t))}{\pi} \tan\left(\frac{\pi z_\gamma^2(t)}{2k_\gamma^2(z_\gamma(t))}\right) + \frac{1}{2\rho_\gamma}\tilde{\Xi}_\gamma^2. \tag{43}$$

Taking the time derivative of L_γ leads to

$$\dot{L}_\gamma = \dot{L}_h + \hbar_\gamma \left(\boldsymbol{\zeta}_\gamma^{\mathrm{T}} \boldsymbol{g}_\gamma \gamma + F_\gamma(\boldsymbol{x}_\gamma) - \frac{\dot{k}_\gamma(t)}{k_\gamma(t)} z_\gamma \right) - \frac{1}{\rho_\gamma} \tilde{\Xi}_\gamma \dot{\hat{\Xi}}_\gamma + \frac{2k_\gamma(t)\dot{k}_\gamma(t)}{\pi} \tan\left(\frac{\pi z_\gamma^2}{2k_\gamma^2(t)} \right), \tag{44}$$

where $\hbar_\gamma = \frac{z_\gamma}{\cos^2\left(\frac{\pi z_\gamma^2}{2k_\gamma^2(t)}\right)}$. $F_\gamma(\boldsymbol{x}_\gamma) = \boldsymbol{\zeta}_\gamma^{\mathrm{T}} \boldsymbol{f}_\gamma + d_\gamma - \dot{\gamma}_d$ collects the unknown dynamics with $\boldsymbol{x}_\gamma = [h, \gamma]^T$.

Construct the virtual control law Q_d and the adaptation law $\dot{\hat{\Xi}}_\alpha$ as

$$\alpha_d = -\frac{1}{\boldsymbol{\zeta}_\gamma^{\mathrm{T}} \boldsymbol{g}_\gamma} \left[\frac{c_\gamma}{\hbar_\gamma} \tan\left(\frac{\pi z_\gamma^2}{2k_\gamma^2(t)} \right) + \frac{\mu_\gamma}{\hbar_\gamma} S_{\gamma 1} + \frac{1}{2}(p+2) \frac{S_{\gamma 2}}{\hbar_\gamma} + \frac{1}{2} \hbar_\gamma \hat{\Xi}_\gamma + M_\gamma z_\gamma + \frac{2k_\gamma(t)\dot{k}_\gamma(t)}{\pi \hbar_\gamma} \tan\left(\frac{\pi z_\gamma^2}{2k_\gamma^2(t)} \right) + \frac{\hbar_h}{\hbar_\gamma} V(z_\gamma + y_\gamma) \right], \tag{45}$$

$$\dot{\hat{\Xi}}_\gamma = \frac{1}{2} \hbar_\gamma^2 \rho_\gamma - \rho_\gamma \hat{\Xi}_\gamma - \rho_\gamma \hat{\Xi}_\gamma^l, \tag{46}$$

where μ_γ, c_γ and ρ_γ are the positive design parameters, $\hat{\Xi}_\gamma$ is the estimate of $\Xi_\gamma = ||\boldsymbol{W}_\gamma^*||^2$ with $\tilde{\Xi}_\gamma = \Xi_\gamma - \hat{\Xi}_\gamma$, the time-varying gain term M_γ is designed similar to (41), and the switching term $S_{\gamma 1}$ and $S_{\gamma 2}$ are designed similar to (39) and (40).

Then, by following similar derivation as step 1, one reaches

$$\dot{L}_\gamma \le -c_h \tan\left(\frac{\pi z_h^2}{2k_h^2(t)} \right) - c_\gamma \tan\left(\frac{\pi z_\gamma^2}{2k_\gamma^2(t)} \right) - \mu_h S_{h1} - \mu_\gamma S_{\gamma 1} - \frac{1}{2}(p+2)(S_{h2} - 1) - \frac{1}{2}(p+2)(S_{\gamma 2} - 1) + \tilde{\Xi}_\gamma \hat{\Xi}_\gamma + \tilde{\Xi}_\gamma \hat{\Xi}_\gamma^l + \hbar_\gamma \boldsymbol{\zeta}_\gamma^{\mathrm{T}} \boldsymbol{g}_\gamma (z_\alpha + y_\alpha). \tag{47}$$

Step 3: Similarly, let us construct the asymmetric time-varying BLF as

$$L_\alpha = L_\gamma + \frac{k_\alpha^2(z_\alpha(t))}{\pi} \tan\left(\frac{\pi z_\alpha^2(t)}{2k_\alpha^2(z_\alpha(t))} \right) + \frac{1}{2\rho_\alpha} \tilde{\Xi}_\alpha^2. \tag{48}$$

Taking the time derivative of L_α leads to

$$\dot{L}_\alpha = \dot{L}_\gamma + \hbar_\alpha \left(\boldsymbol{\zeta}_\alpha^{\mathrm{T}} \boldsymbol{g}_\alpha \alpha + F_\alpha(\boldsymbol{x}_\alpha) - \frac{\dot{k}_\alpha(t)}{k_\alpha(t)} z_\alpha \right) - \frac{1}{\rho_\alpha} \tilde{\Xi}_\alpha \dot{\hat{\Xi}}_\alpha + \frac{2k_\alpha(t)\dot{k}_\alpha(t)}{\pi} \tan\left(\frac{\pi z_\alpha^2}{2k_\alpha^2(t)} \right), \tag{49}$$

where $\hbar_\alpha = \frac{z_\alpha}{\cos^2\left(\frac{\pi z_\alpha^2}{2k_\alpha^2(t)}\right)}$. $F_\alpha(\boldsymbol{x}_\alpha) = \boldsymbol{\zeta}_\alpha^{\mathrm{T}} \boldsymbol{f}_\alpha + d_\alpha - \dot{\alpha}_d$ collects the unknown dynamics with $\boldsymbol{x}_\alpha = [h, \gamma, \alpha]^T$.

Construct the virtual control law Q_d and the adaptation law $\dot{\hat{\Xi}}_\alpha$ as

$$Q_d = -\frac{1}{\boldsymbol{\zeta}_\alpha^{\mathrm{T}} \boldsymbol{g}_\alpha} \left[\frac{c_\alpha}{\hbar_\alpha} \tan\left(\frac{\pi z_\alpha^2}{2k_\alpha^2(t)} \right) + \frac{\mu_\alpha}{\hbar_\alpha} S_{\alpha 1} + \frac{1}{2}(p+2) \frac{S_{\alpha 2}}{\hbar_\alpha} + \frac{1}{2} \hbar_\alpha \hat{\Xi}_\alpha + \frac{2k_\alpha(t)\dot{k}_\alpha(t)}{\pi \hbar_\alpha} \tan\left(\frac{\pi z_\alpha^2}{2k_\alpha^2(t)} \right) + M_\alpha z_\alpha + \frac{\hbar_\gamma}{\hbar_\alpha} \boldsymbol{\zeta}_\gamma^{\mathrm{T}} \boldsymbol{g}_\gamma (z_\alpha + y_\alpha) \right], \tag{50}$$

$$\dot{\hat{\Xi}}_\alpha = \frac{1}{2} \hbar_\alpha^2 \rho_\alpha - \rho_\alpha \hat{\Xi}_\alpha - \rho_\alpha \hat{\Xi}_\alpha^l, \tag{51}$$

where μ_α, c_α and ρ_α are the positive design parameters, $\hat{\Xi}_\alpha$ is the estimate of $\Xi_\alpha = ||\boldsymbol{W}_\alpha^*||^2$ with $\tilde{\Xi}_\alpha = \Xi_\alpha - \hat{\Xi}_\alpha$, the time-varying gain term M_α is designed similar to (41), and the switching term $S_{\alpha 1}$ and $S_{\alpha 2}$ are designed similar to (39) and (40). Then, the time derivative of L_α reaches

$$\dot{L}_\alpha \le -c_h \tan\left(\frac{\pi z_h^2}{2k_h^2(t)} \right) - c_h \tan\left(\frac{\pi z_\gamma^2}{2k_\gamma^2(t)} \right) - c_\alpha \tan\left(\frac{\pi z_\alpha^2}{2k_\alpha^2(t)} \right) - \mu_h S_{h1} - \mu_\gamma S_{\gamma 1} - \mu_\alpha S_{\alpha 1} - \frac{1}{2}(p+2)(S_{h2} - 1) - \frac{1}{2}(p+2)(S_{\gamma 2} - 1) - \frac{1}{2}(p+2)(S_{\alpha 2} - 1) + \tilde{\Xi}_\gamma \hat{\Xi}_\gamma + \tilde{\Xi}_\alpha \hat{\Xi}_\alpha + \tilde{\Xi}_\gamma \hat{\Xi}_\gamma^l + \tilde{\Xi}_\alpha \hat{\Xi}_\alpha^l + \hbar_\alpha \boldsymbol{\zeta}_\alpha^{\mathrm{T}} \boldsymbol{g}_\alpha (z_Q + y_Q). \tag{52}$$

Step 4: Similar to step 1, let us construct the asymmetric time-varying BLF as

$$L_Q = L_\alpha + \frac{k_Q^2(z_Q(t))}{\pi} \tan\left(\frac{\pi z_Q^2(t)}{2k_Q^2(z_Q(t))} \right) + \frac{1}{2\rho_Q} \tilde{\Xi}_Q^2. \tag{53}$$

Taking the time derivative of L_Q results in

$$\dot{L}_Q = \dot{L}_\alpha + \hbar_Q \left(\boldsymbol{\zeta}_Q^{\mathrm{T}} \boldsymbol{g}_Q \delta_e + F_Q(\boldsymbol{x}_Q) - \dot{e}_Q - \frac{\dot{k}_Q(t)}{k_Q(t)} z_Q \right) - \frac{1}{\rho_Q} \tilde{\Xi}_Q \dot{\hat{\Xi}}_Q + \frac{2k_Q(t)\dot{k}_Q(t)}{\pi} \tan\left(\frac{\pi z_Q^2}{2k_Q^2(t)} \right), \tag{54}$$

where $\hbar_Q = \frac{z_Q}{\cos^2\left(\frac{\pi z_Q^2}{2k_Q^2(t)}\right)}$. $F_Q(\boldsymbol{x}_Q) = \boldsymbol{\zeta}_Q^{\mathrm{T}} \boldsymbol{f}_Q + d_Q - \dot{Q}_d - \dot{y}_Q$ collects the unknown dynamics with $\boldsymbol{x}_Q = [h, \gamma, \alpha, Q]^T$.

Similar to Steps 1-3, let us construct the actual control law $\delta_{e,c}$, adaptation law $\dot{\hat{\Xi}}_Q$, and auxiliary variable $\dot{e}_Q$ as

$$\delta_{e,c} = -\frac{1}{\boldsymbol{\zeta}_Q^{\mathrm{T}} \boldsymbol{g}_Q} \left[\frac{c_Q}{\hbar_Q} \tan\left(\frac{\pi z_Q^2}{2k_Q^2(t)} \right) + \frac{\mu_Q}{\hbar_Q} S_{Q1} + \frac{1}{2}(p+2) \frac{S_{Q2}}{\hbar_Q} + \frac{1}{2} \hbar_Q \hat{\Xi}_Q + M_Q \tilde{Q} + \frac{2k_Q(t)\dot{k}_Q(t)}{\pi \hbar_Q} \tan\left(\frac{\pi z_Q^2}{2k_Q^2(t)} \right) + \frac{\hbar_\alpha}{\hbar_Q} \boldsymbol{\zeta}_\alpha^{\mathrm{T}} \boldsymbol{g}_\alpha (z_Q + y_Q) \right], \tag{55}$$

$$\dot{\hat{\Xi}}_Q = -\rho_Q \hat{\Xi}_Q - \rho_Q \hat{\Xi}_Q^l + \frac{1}{2} \hbar_Q^2 \rho_Q, \tag{56}$$

$$\dot{e}_Q = -M_Q e_Q + \boldsymbol{\zeta}_Q^{\mathrm{T}} \boldsymbol{g}_Q (\delta_e - \delta_{e,c}), \tag{57}$$

where $\mu_Q > 0, c_Q > 0$ and $\rho_Q > 0$ are design parameters, $\hat{\Xi}_Q$ is the estimate of $\Xi_Q = ||\boldsymbol{W}_Q^*||^2$ with $\tilde{\Xi}_Q = \Xi_Q - \hat{\Xi}_Q$, the time-varying gain term M_Q is designed similar to (41), and the switching term S_{Q1} and S_{Q2} are designed similar to (39) and (40). Then, the time derivative of L_Q can be bounded by

$$\begin{aligned}\dot{L}_Q \leq & -c_h \tan\left(\frac{\pi z_h^2}{2k_h^2(t)}\right) - c_\gamma \tan\left(\frac{\pi z_\gamma^2}{2k_\gamma^2(t)}\right) - c_\alpha \tan\left(\frac{\pi z_\alpha^2}{2k_\alpha^2(t)}\right) \\ & - c_Q \tan\left(\frac{\pi z_Q^2}{2k_Q^2(t)}\right) - \mu_h S_{h1} - \mu_\gamma S_{\gamma 1} - \mu_\alpha S_{\alpha 1} - \mu_Q S_{Q1} \\ & - \frac{1}{2}(p+2)(S_{h2}-1) - \frac{1}{2}(p+2)(S_{\gamma 2}-1) + \tilde{\Xi}_\gamma \hat{\Xi}_\gamma \\ & - \frac{1}{2}(p+2)(S_{\alpha 2}-1) - \frac{1}{2}(p+2)(S_{Q2}-1) + \tilde{\Xi}_\alpha \hat{\Xi}_\alpha \\ & + \tilde{\Xi}_Q \hat{\Xi}_Q + \tilde{\Xi}_\gamma \hat{\Xi}_\gamma^l + \tilde{\Xi}_\alpha \hat{\Xi}_\alpha^l + \tilde{\Xi}_Q \hat{\Xi}_Q^l. \end{aligned} \tag{58}$$

IV. Stability Analysis

Theorem 1: Consider the closed-loop system composed by (1)-(12), by the control laws (23), (38), (45), (50) and (55), by the filters (37), and by the parameter adaptation laws (28), (46), (51) and (56). Let Assumption 1 hold. Consider any initial conditions satisfying $L(0) \leq \Delta_1$, $z_\star(0) \in (k_{a_\star}, k_{b_\star})$ where $\Delta_1 > \max\{k_{a_\star}, k_{b_\star}\}$ is a positive constant. Then, it holds that:

- all closed-loop signals including $z_\star$, $\tilde{\Xi}_V$, $\tilde{\Xi}_\gamma$, $\tilde{\Xi}_\alpha$, $\tilde{\Xi}_Q$, y_γ, y_α, and y_Q are semi-globally-uniformly-ultimately-bounded, and converge to some residual sets (as shown in (72)) in finite-time $\overline{T} \leq \frac{1}{\kappa_1(1-l)} \ln\left((2\kappa_1 L^{1-l}(0) + \kappa_2)/\kappa_2\right)$.
- the state errors $z_\star$ will stay in the asymmetric time-varying compact sets $\Omega_\star = \{z_\star : k_{a_\star}(t) \leq z_\star \leq k_{b_\star}(t)\}$ all the time.

Proof. See Appendix. ■

Remark 3: Note that only four scalar parameter adaptation laws (28), (46), (51) and (56) and two scalar first-order filters (37) are involved in our design, which makes it simpler than vector-based adaptation laws in backstepping approach proposed for HFVs [14]. In addition, the proposed switching mechanism can be simply implemented as a static nonlinearity as in (39) and (40), which is comparable to the complexity of state-of-the-art approaches proposed for HFVs, such as sliding mode control design [17].

Remark 4: The role of the auxiliary dynamic systems (27) and (57) is to compensate for the command errors $\boldsymbol{\zeta}_V^{\mathrm{T}} \boldsymbol{g}_V(\Phi - \Phi_c)$ and $\boldsymbol{\zeta}_Q^{\mathrm{T}} \boldsymbol{g}_Q(\delta_e - \delta_{e,c})$ which arise due to the presence of magnitude, bandwidth, and rate constraints, as in Fig. 2. It is worth remarking that we are not aware of control method for HFVs that can handle actuator constraints and asymmetric time-varying constraints in the framework of finite-time stability in a provably stable way.

V. Simulation Results

In this section, a simple case study is first given to show that singularity issue occurs in conventional finite-time schemes, whereas our proposed switching mechanism avoids such issue. Then, we compare our method with the HFV designs [17] and [29] to illustrate the effectiveness of the proposed strategy over existing methods in terms of convergence, smoothness and constraints satisfaction.

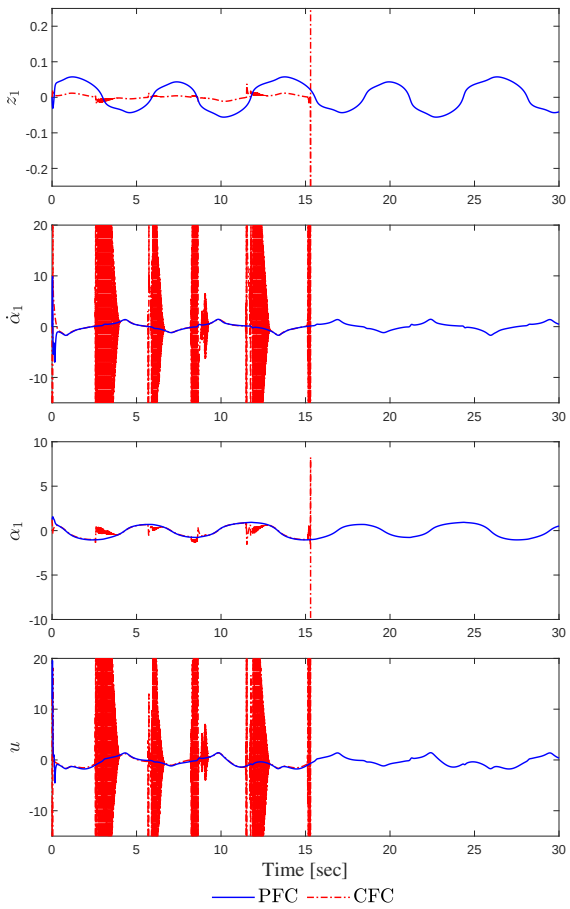

Fig. 3: Curves of closed-loop signals of two control methods.

A. Case Study

Consider a second-order nonlinear system

$$\dot{x}_1 = x_2 + x_1 + x_2^3, \quad \dot{x}_2 = u + x_1^2 x_2^2, \quad y = x_1, \tag{59}$$

where $x_1, x_2 \in \mathbb{R}$ represent the state variables, $u \in \mathbb{R}$ is the control input, $y \in \mathbb{R}$ is the system output, and the desired trajectory is $y_d = \sin t + 0.5\sin(0.5t)$.

Define the tracking errors $z_1 = x_1 - y_d$ and $z_2 = x_2 - \alpha_1$, where α_1 is the virtual control law. In what follows, we do not take into account state constraints in control design for the purpose of highlighting the singularity issue. Therefore, our proposed finite-time switching control laws (PFC) and conventional finite-time control laws (CFC) [21]-[24] can be given in (60) and (61), respectively.

$$\text{PFC}: \begin{cases} \alpha_1 = -c_1 z_1 - \mu_1 S_{1,1}(z_1) + \dot{y}_d, \\ u = -c_2 z_2 - \mu_2 S_{2,1}(z_2) + \dot{\alpha}_1, \end{cases} \tag{60}$$

$$\text{CFC}: \begin{cases} \alpha_1 = -c_1 z_1 - \mu_1 z_1^l + \dot{y}_d, \\ u = -c_2 z_2 - \mu_2 z_2^l + \dot{\alpha}_1, \end{cases} \tag{61}$$

TABLE I: The control structures of CFC, and CIC.

Control laws of CFC

$$\Phi = \frac{1}{\boldsymbol{\zeta}_V^{\mathrm{T}}\boldsymbol{g}_V}\Big(- l_V \mathrm{sig}^l(z_V) - \boldsymbol{\zeta}_V^{\mathrm{T}}\boldsymbol{f}_V + \dot{V}_r - \lambda_V \mathrm{sgn}(S_V)\Big),$$

$$\delta_e = \frac{1}{\boldsymbol{\zeta}_Q^{\mathrm{T}}\boldsymbol{g}_Q}\Big(- l_Q \mathrm{sig}^l(z_Q) - \boldsymbol{\zeta}_Q^{\mathrm{T}}\boldsymbol{f}_Q + \dot{Q}_d - \lambda_Q \mathrm{sgn}(S_Q)\Big),$$

where $\mathrm{sig}^l(z_i) = \mathrm{sgn}(z_i)\cdot|z_i|^l$, $S_i = z_i + \int_0^t l_i \mathrm{sig}^l(z_i)\mathrm{d}\tau$, $i \in \{V, Q\}$.

Control laws of CIC

$$\Phi = - c_V z_V - 0.5\int z_V(t)\mathrm{d}t - \frac{\mathrm{d}z_V(t)}{\mathrm{d}t},$$

$$\delta_e = \frac{1}{\hat{g}_3}\Big[- \hat{\omega}_3^T\theta_3(\bar{x}_3) - c_Q e_Q - \frac{e_\theta}{\psi} + \dot{\kappa}_{3c} - \hat{\tau}_{3m}\tanh\Big(\frac{e_\theta}{0.75}\Big)\Big],$$

where $\dot{\hat{\omega}}_3 = (e_Q + \tilde{x}_3)\theta_3(\bar{x}_3) - 0.5\hat{\omega}_3$.

TABLE II: Performance indices of control inputs.

Control inputs	PFC	CFC	CIC
Φ	0.2452	0.3971	0.3824
δ_e	6.9437	9.3950	9.9032
$\dot{\Phi}$	0.0102	0.0119	0.0121
$\dot{\delta}_e$	0.0032	0.0055	0.0049

where c_1, c_2, μ_1, and μ_2 are positive design parameters, and

$$S_{i,1} = \begin{cases} z_i^l, & \text{if } |z_i| \geq \tau_i, \\ v_i z_i + o_i z_i^3, & \text{else,} \end{cases}$$

with $v_i = \frac{(3-l)}{2}\tau_i^{l-1}$, $o_i = \frac{(l-1)}{2}\tau_i^{l-3}$, $i = 1, 2$.

In simulation, the design parameters are chosen as $c_1 = c_2 = 5$, $\mu_1 = \mu_2 = 15$, $l = 0.6$, and $\tau_1 = \tau_2 = 0.1$. Simulation results are given in Fig. 3. Due to the presence of $\dot{\alpha}_1$ in u, it can be seen from Fig. 3 that, under conventional finite-time control laws, singularity issues occur at 2.57s, 5.71s, 8.65s, 11.53s, and 15.31s, while our proposed finite-time switching control law circumvents such issues.

B. Application to the HFVs Dynamics

Comparative simulations are carried out among the proposed PFC, the conventional finite-time nonsingular terminal sliding mode unconstrained control (CFC [17]), and the conventional infinite-time constrained control (CIC [29]), whose controllers are listed in Table I. In this simulation, the vehicle climbs a maneuver from initial values $h = 88,000$ ft and $V = 7700$ ft/s to final values $h = 91,000$ ft and $V = 8700$ ft/s, respectively. The HFVs model parameter values are borrowed from [7], and the upper and lower thresholds are set as $k_{a_V} = -1.15\exp(-0.2t) - 0.05$, $k_{b_V} = 0.15\exp(-0.2t) + 0.05$, $k_{a_h} = -2.4\exp(-0.2t) - 0.1$, $k_{b_h} = 0.1\exp(-0.2t) + 0.1$, $k_{a_\gamma} = k_{a_\alpha} = k_{a_Q} = -0.0048\exp(-0.2t) - 0.0002$, $k_{b_\gamma} = k_{b_Q} = 0.0008\exp(-0.2t) + 0.0002$, and $k_{b_\alpha} = 0.0018\exp(-0.2t) + 0.0002$. The control parameters are chosen as $c_V = 5$, $\mu_V = 1$, $p = 5$, $o_V = o_\gamma = o_\alpha = o_Q = 0.1$, $a_{h1} = 10$, $a_{h2} = 1$, $c_\gamma = 5$, $\mu_\gamma = 1$, $c_\alpha = 10$, $\mu_\alpha = 2$, $c_Q = 40$, $\mu_Q = 5$, $l = 0.6$, $\tau_V = 0.01$, and $\tau_\gamma = \tau_\alpha = \tau_Q = 0.001$. Parameters for adaptive laws are set as $\rho_V = 0.5$, $\rho_\gamma = \rho_\alpha = \rho_Q = 0.75$. The positive filter parameters are selected as $\tau_{\alpha 1} = \tau_{Q1} = 5$ and $\tau_{\alpha 2} = \tau_{Q2} = 2.5$. The initial state variables are set as $V(0) = 7699$ ft/s, $h(0) = 87998$ ft, $\gamma(0) = 0$ deg, $\alpha(0) = 1.6325$ deg, and $Q(0) = 0$ deg/s, and the initial values of $\hat{\Xi}_V$, $\hat{\Xi}_\gamma$, $\hat{\Xi}_\alpha$, and $\hat{\Xi}_Q$ are selected as zero. Specifically, the uncertain aerodynamic coefficients are modelled as $C_i = C_i^*(1 + \Delta_i)$, where C_i^* represents the nominal coefficient and Δ_i represents the uncertain factor ranging from -30% to 30%. Parameters for actuator dynamics are set as $\omega_n = 5\,\mathrm{rad/s}$ and $\zeta = 0.95$. Based on practical engineering characteristics, the limitations of the actuators of HFVs are set as $\Phi \in [0.05, 1.5]$, $\dot{\Phi} \in [-1, 1]$, $\delta_e \in [-20\ \mathrm{deg}, 20\ \mathrm{deg}]$, and $\dot{\delta}_e \in [-20\ \mathrm{deg/s}, 20\ \mathrm{deg/s}]$.

The fuzzy rules in $\boldsymbol{W}_V^{*\mathrm{T}}\boldsymbol{\varphi}_V(\boldsymbol{x}_V)$ are listed as

$\mathcal{R}^l$: If V is F_V^i, then y is B^l, where $i = 1, 2, 3$; $l = 1, 2, 3$.

The fuzzy rules in $\boldsymbol{W}_\gamma^{*\mathrm{T}}\boldsymbol{\varphi}_\gamma(\boldsymbol{x}_\gamma)$ are listed as

$\mathcal{R}^l$: If γ is F_γ^j, then y is B^l, where $j = 1, 2, 3$; $l = 1, 2, \ldots, 9$.

The fuzzy rules in $\boldsymbol{W}_\alpha^{*\mathrm{T}}\boldsymbol{\varphi}_\alpha(\boldsymbol{x}_\alpha)$ are listed as

$\mathcal{R}^l$: If γ is F_γ^j, and α is F_α^k, then y is B^l, where $j = 1, 2, 3$; $k = 1, 2, 3$; $l = 1, 2, \ldots, 27$.

The fuzzy rules in $\boldsymbol{W}_Q^{*\mathrm{T}}\boldsymbol{\varphi}_Q(\boldsymbol{x}_Q)$ are listed as

$\mathcal{R}^l$: If γ is F_γ^j, and α is F_α^k, and Q is F_Q^p, then y is B^l, where $j = 1, 2, 3$; $k = 1, 2, 3$; $p = 1, 2, 3$; $l = 1, 2, \ldots, 81$.

Simulation results are given in Figs. 4-5. It can be seen from Fig. 4 and Fig. 5 (h)-(j) that our proposed method exhibits a faster convergence rate and a smaller steady state tracking error for both velocity and altitude channels, while guaranteeing the satisfaction of asymmetric time-varying constraints. From Fig. 5 (a)-(b), it can be observed that our proposed method not only satisfies actuator constraints, but displays a smoother response and a smaller magnitude than CFC and CIC. Fig. 5 (c)-(g) show the boundedness of flight state variables γ, α, Q, η_1, and η_2 of PFC, CFC, and CIC. In Tables II-III, the tracking performances of PFC, CFC, and CIC are quantified via several performance indices: integral absolute error (IAE) $\big[\int_0^T |e(t)|\mathrm{d}t\big]$, integral time absolute error (ITAE) $\big[\int_0^T t|e(t)|\mathrm{d}t\big]$, root mean square error (RMSE) $\big[\frac{1}{T}\int_0^T e^2(t)\mathrm{d}t\big]^{\frac{1}{2}}$, and mean absolute error (MAE) $\big[\frac{1}{T}\int_0^T |e(t)|\mathrm{d}t\big]$. In addition, the control indexes are defined as the mean absolute control actions (MACA) $\Big[\frac{1}{T}\int_0^T |\Phi|\mathrm{d}t\Big]$, $\big[\frac{1}{T}\int_0^T |\dot{\Phi}|\mathrm{d}t\big]$, $\big[\frac{1}{T}\int_0^T |\delta_e|\mathrm{d}t\big]$, and $\big[\frac{1}{T}\int_0^T |\dot{\delta}_e|\mathrm{d}t\big]$. Tables II-III show that the control effort of PFC is smaller than the one of CFC and CIC and that the performance indexes of PFC are smaller than those of CFC and CIC, which show that the proposed design scores better than the state of the art in terms of tracking performance, control effort and smoothness.

VI. Conclusion

A novel fuzzy adaptive design is constructed for HFVs in spite of asymmetric time-varying constraints and actuator constraints. It is shown that the proposed differentiable smooth

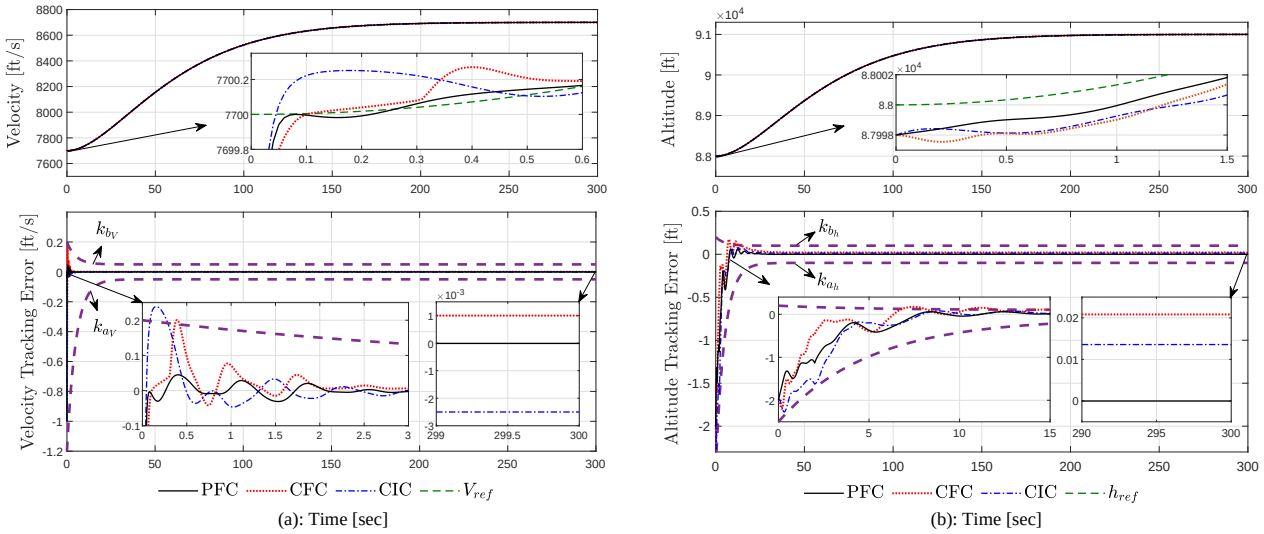

Fig. 4: (a) Velocity tracking performance; (b) Altitude tracking performance.

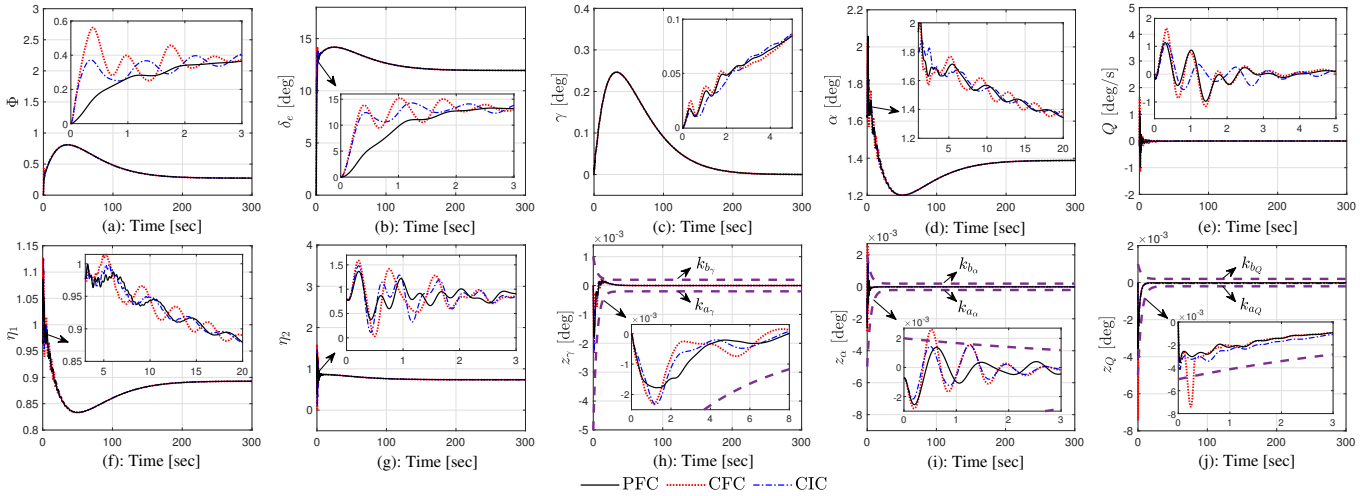

Fig. 5: (a) Fuel equivalence ratio Φ; (b) Elevator angular deflection δ_e; (c) FPA γ; (d) AOA α; (e) Pitch rate Q; (f) First generalized flexible coordinate η_1; (g) Second generalized flexible coordinate η_2; (h) FPA tracking error z_γ; (i) AOA tracking error z_α; (j) Pitch rate tracking error z_Q.

adaptive fuzzy controller can ensure finite-time convergence with the aid of a smooth switch between a fractional and a linear control. Tan-type BLFs are incorporated into the design to guarantee the satisfaction of asymmetric time-varying constraints imposed on flight state variables. Auxiliary systems are constructed to counteract the adverse effects caused by actuator physical constraints. It is worth investigating how the proposed method can be adopted in a distributed control setting like in [44]-[45], where the multiple HFVs have to minimize a consensus error in place of a tracking error.

APPENDIX

PROOF OF THEOREM 1

Construct the entire Lyapunov function

$$L = \bar{L}_V + L_Q + \frac{y_\gamma^2}{2} + \frac{y_\alpha^2}{2} + \frac{y_Q^2}{2}, \tag{62}$$

where $L_y = \frac{y_\gamma^2}{2} + \frac{y_\alpha^2}{2} + \frac{y_Q^2}{2}$.

The time derivative of L_y is

$$\begin{aligned}\dot{L}_y \leq\ & y_Q \iota_Q \left(z_\alpha, \dot{z}_\alpha, k_\alpha(t), \dot{k}_\alpha(t), \ddot{k}_\alpha(t), \hat{\Xi}_\gamma, \hat{\Xi}_\alpha, y_\gamma, y_\alpha, y_Q\right) \\ & + y_\alpha \iota_\alpha \left(z_\gamma, \dot{z}_\gamma, k_\gamma(t), \dot{k}_\gamma(t), \ddot{k}_\gamma(t), \hat{\Xi}_\gamma, y_\gamma, y_\alpha\right) \\ & + y_\gamma \iota_\gamma (z_h, \dot{z}_h, k_h(t), \dot{k}_h(t), \ddot{k}_h(t), \dot{h}_{ref}, \ddot{h}_{ref}) \\ & - \tau_{\gamma 2} y_\gamma^{l+1} - \tau_{\gamma 1} y_\gamma^2 - \frac{\bar{g}_\gamma^2 \tau_{\alpha 2} y_\alpha^{l+1}}{\underline{g}_\gamma} - \frac{\bar{g}_\gamma^2 \tau_{\alpha 1} y_\alpha^2}{\underline{g}_\gamma} \\ & - \tau_{Q2} y_Q^{l+1} - \tau_{Q1} y_Q^2. \end{aligned} \tag{63}$$

Define a compact set as $\Omega_n = \{(z_h, \dot{z}_h, z_\gamma, \dot{z}_\gamma, z_\alpha, \dot{z}_\alpha, k_h(t), \dot{k}_h(t), \ddot{k}_h(t), k_\gamma(t), \dot{k}_\gamma(t), \ddot{k}_\gamma(t), k_\alpha(t), \dot{k}_\alpha(t), \ddot{k}_\alpha(t), \hat{\Xi}_\gamma, \hat{\Xi}_\alpha, y_\gamma, y_\alpha, y_Q)\}$, with Δ_1 being a positive constant. If $L(t) \leq \Delta_1$, together with Assumption 1, it can be obtained

TABLE III: Performance indices of velocity and altitude channels for the three designs.

Performance Indices	Velocity Channel			Altitude Channel		
	PFC	CFC	CIC	PFC	CFC	CIC
IAE	0.0602	0.1975	0.1603	10.5238	17.4467	16.9052
ITAE	0.5220	8.3307	6.0020	233.8438	523.4490	602.7337
RMSE	0.0040	0.0055	0.0045	0.1020	0.1270	0.1022
MAE	$4.3277*10^{-5}$	$2.0448*10^{-4}$	$1.9667*10^{-4}$	0.0095	0.0123	0.0119

that there always exists a positive constant $\Lambda_\star$ such that $\iota_\star(\cdot)\leq\Lambda_\star$ on the compact set $\Omega_n\times\Omega_{ref}$ with $\star$ standing for γ, α, and Q. By applying Young's inequality and combining (33) with (58), the derivative of L is derived as

$$\begin{aligned}\dot{L}\leq&-c_V\tan\left(\frac{\pi z_V^2}{2k_V^2(t)}\right)-c_h\tan\left(\frac{\pi z_h^2}{2k_h^2(t)}\right)-c_\gamma\tan\left(\frac{\pi z_\gamma^2}{2k_\gamma^2(t)}\right)\\&-c_\alpha\tan\left(\frac{\pi z_\alpha^2}{2k_\alpha^2(t)}\right)-c_Q\tan\left(\frac{\pi z_Q^2}{2k_Q^2(t)}\right)-\mu_V S_{V1}-\mu_h S_{h1}\\&-\mu_\gamma S_{\gamma1}-\mu_\alpha S_{\alpha1}-\mu_Q S_{Q1}-\frac{1}{2}(p+2)(S_{V2}-1)-\widehat{\tau}_{\gamma1}y_\gamma^2\\&-\frac{1}{2}(p+2)(S_{h2}-1)-\frac{1}{2}(p+2)(S_{\gamma2}-1)-\widehat{\tau}_{\alpha1}y_\alpha^2\\&-\frac{1}{2}(p+2)(S_{\alpha2}-1)-\frac{1}{2}(p+2)(S_{Q2}-1)-\widehat{\tau}_{Q1}y_Q^2\\&-\tau_{\gamma2}y_\gamma^{l+1}-\tau_{\alpha2}y_\alpha^{l+1}-\tau_{Q2}y_Q^{l+1}+\tilde{\Xi}_V\hat{\Xi}_V+\tilde{\Xi}_\gamma\hat{\Xi}_\gamma+\tilde{\Xi}_\alpha\hat{\Xi}_\alpha\\&+\tilde{\Xi}_Q\hat{\Xi}_Q+\tilde{\Xi}_V\hat{\Xi}_V^l+\tilde{\Xi}_\gamma\hat{\Xi}_\gamma^l+\tilde{\Xi}_\alpha\hat{\Xi}_\alpha^l+\tilde{\Xi}_Q\hat{\Xi}_Q^l,\end{aligned}\tag{64}$$

where $\widehat{\tau}_{\gamma1}=\tau_{\gamma1}-1/(2\chi_\gamma)$, $\widehat{\tau}_{\alpha1}=\tau_{\alpha1}-1/(2\chi_\alpha)$, $\widehat{\tau}_{Q1}=\tau_{Q1}-1/(2\chi_Q)$ and $d=\chi_\gamma\Lambda_\gamma^2/2+\chi_\alpha\Lambda_\alpha^2/2+\chi_Q\Lambda_Q^2/2$ with χ_γ, χ_α, χ_Q being positive constants. Here we choose $\tau_{\gamma1}>1/(2\chi_\gamma)$, $\tau_{\alpha1}>1/(2\chi_\alpha)$ and $\tau_{Q1}>1/(2\chi_Q)$ such that $\widehat{\tau}_{\gamma1}>0$, $\widehat{\tau}_{\alpha1}>0$ and $\widehat{\tau}_{Q1}>0$. According to Lemmas 1-2, we have

$$\tilde{\Xi}_\star\hat{\Xi}_\star\leq\Xi_\star^2-\frac{1}{2}\tilde{\Xi}_\star^2,\ \tilde{\Xi}_\star\hat{\Xi}_\star^l\leq\frac{1}{1+l}\left(2\Xi_\star^{1+l}-\left(\tilde{\Xi}_\star^2\right)^{\frac{1+l}{2}}\right).\tag{65}$$

Then the inequation (64) can be rewritten as

$$\begin{aligned}\dot{L}\leq&-\frac{1}{1+l}\left[\left(\tilde{\Xi}_V^2\right)^{\frac{1+l}{2}}+\left(\tilde{\Xi}_\gamma^2\right)^{\frac{1+l}{2}}+\left(\tilde{\Xi}_\alpha^2\right)^{\frac{1+l}{2}}+\left(\tilde{\Xi}_Q^2\right)^{\frac{1+l}{2}}\right]\\&-c_V\tan\left(\frac{\pi z_V^2}{2k_V^2(t)}\right)-c_h\tan\left(\frac{\pi z_h^2}{2k_h^2(t)}\right)-c_\gamma\tan\left(\frac{\pi z_\gamma^2}{2k_\gamma^2(t)}\right)\\&-c_\alpha\tan\left(\frac{\pi z_\alpha^2}{2k_\alpha^2(t)}\right)-c_Q\tan\left(\frac{\pi z_Q^2}{2k_Q^2(t)}\right)-\mu_V S_{V1}-\mu_h S_{h1}\\&-\mu_\gamma S_{\gamma1}-\mu_\alpha S_{\alpha1}-\mu_Q S_{Q1}-\frac{1}{2}(p+2)(S_{V2}-1)-\widehat{\tau}_{\gamma1}y_\gamma^2\\&-\frac{1}{2}(p+2)(S_{h2}-1)-\frac{1}{2}(p+2)(S_{\gamma2}-1)-\widehat{\tau}_{\alpha1}y_\alpha^2\\&-\frac{1}{2}(p+2)(S_{\alpha2}-1)-\frac{1}{2}(p+2)(S_{Q2}-1)-\widehat{\tau}_{Q1}y_Q^2\\&-\tau_{\gamma2}y_\gamma^{l+1}-\tau_{\alpha2}y_\alpha^{l+1}-\tau_{Q2}y_Q^{l+1}-\frac{1}{2}\tilde{\Xi}_V^2-\frac{1}{2}\tilde{\Xi}_\gamma^2-\frac{1}{2}\tilde{\Xi}_\alpha^2\\&-\frac{1}{2}\tilde{\Xi}_Q^2+d.\end{aligned}\tag{66}$$

where $d=\frac{2}{1+l}\left(\Xi_V^{1+l}+\Xi_\gamma^{1+l}+\Xi_\alpha^{1+l}+\Xi_Q^{1+l}\right)+\Xi_V^2+\Xi_\gamma^2+\Xi_\alpha^2+\Xi_Q^2$. From the definition of switching functions (39) and (40), the following two cases should be considered.

Case 1: When $|z_\star|<\tau_\star$, we have the derivative of L as

$$\begin{aligned}\dot{L}\leq&-\left[c_V+\mu_V\tan^{l-1}\left(\frac{\pi\tau_V^2}{2k_V^2(t)}\right)\right]\tan\left(\frac{\pi z_V^2}{2k_V^2(t)}\right)-\frac{1}{2}\tilde{\Xi}_V^2\\&-\left[c_\gamma+\mu_\gamma\tan^{l-1}\left(\frac{\pi\tau_\gamma^2}{2k_\gamma^2(t)}\right)\right]\tan\left(\frac{\pi z_\gamma^2}{2k_\gamma^2(t)}\right)-\frac{1}{2}\tilde{\Xi}_\gamma^2\\&-\left[c_\alpha+\mu_\alpha\tan^{l-1}\left(\frac{\pi\tau_\alpha^2}{2k_\alpha^2(t)}\right)\right]\tan\left(\frac{\pi z_\alpha^2}{2k_\alpha^2(t)}\right)-\frac{1}{2}\tilde{\Xi}_\alpha^2\\&-\left[c_Q+\mu_Q\tan^{l-1}\left(\frac{\pi\tau_Q^2}{2k_Q^2(t)}\right)\right]\tan\left(\frac{\pi z_Q^2}{2k_Q^2(t)}\right)-\frac{1}{2}\tilde{\Xi}_Q^2\\&-\left[c_h+\mu_h\tan^{l-1}\left(\frac{\pi\tau_h^2}{2k_h^2(t)}\right)\right]\tan\left(\frac{\pi z_h^2}{2k_h^2(t)}\right)-\widehat{\tau}_{\gamma1}y_\gamma^2\\&-\widehat{\tau}_{\alpha1}y_\alpha^2-\widehat{\tau}_{Q1}y_Q^2+d.\end{aligned}\tag{67}$$

Noting (67), we also have

$$\dot{L}\leq-\varpi L+d,\tag{68}$$

in which $\varpi=\min\left\{\frac{\pi}{k_\star(t)}\left[c_\star+\mu_\star\tan^{l-1}\left(\frac{\pi\tau_\star^2}{2k_\star^2(t)}\right)\right],\rho_\star,2\widehat{\tau}_{\star1}\right\}$. Integrating (68) over $[0,t]$, we have

$$L(t)\leq\left(L(0)-\frac{d}{\varpi}\right)e^{-\varpi t}+\frac{d}{\varpi}.\tag{69}$$

This fact implies that all closed-loop signals are bounded.

Case 2: When $|z_\star|\geq\tau_\star$, we have the derivative of L as

$$\begin{aligned}\dot{L}\leq&-\frac{1}{1+l}\left[\left(\tilde{\Xi}_V^2\right)^{\frac{1+l}{2}}+\left(\tilde{\Xi}_\gamma^2\right)^{\frac{1+l}{2}}+\left(\tilde{\Xi}_\alpha^2\right)^{\frac{1+l}{2}}+\left(\tilde{\Xi}_Q^2\right)^{\frac{1+l}{2}}\right]\\&-\mu_V\tan\left(\frac{\pi z_V^2}{2k_V^2(t)}\right)-\mu_V\tan^l\left(\frac{\pi z_V^2}{2k_V^2(t)}\right)-\frac{1}{2}\tilde{\Xi}_V^2\\&-\mu_\gamma\tan\left(\frac{\pi z_\gamma^2}{2k_\gamma^2(t)}\right)-\mu_\gamma\tan^l\left(\frac{\pi z_\gamma^2}{2k_\gamma^2(t)}\right)-\frac{1}{2}\tilde{\Xi}_\gamma^2\\&-\mu_\alpha\tan\left(\frac{\pi z_\alpha^2}{2k_\alpha^2(t)}\right)-\mu_\alpha\tan^l\left(\frac{\pi z_\alpha^2}{2k_\alpha^2(t)}\right)-\frac{1}{2}\tilde{\Xi}_\alpha^2\\&-\mu_Q\tan\left(\frac{\pi z_Q^2}{2k_Q^2(t)}\right)-\mu_Q\tan^l\left(\frac{\pi z_Q^2}{2k_Q^2(t)}\right)-\frac{1}{2}\tilde{\Xi}_Q^2\\&-\mu_h\tan\left(\frac{\pi z_h^2}{2k_h^2(t)}\right)-\mu_h\tan^l\left(\frac{\pi z_h^2}{2k_h^2(t)}\right)-\widehat{\tau}_{\gamma1}y_\gamma^2\\&-\widehat{\tau}_{\alpha1}y_\alpha^2-\widehat{\tau}_{Q1}y_Q^2-\tau_{\gamma2}y_\gamma^{l+1}-\tau_{\alpha2}y_\alpha^{l+1}-\tau_{Q2}y_Q^{l+1}+d.\end{aligned}\tag{70}$$

It then follows from (70) that

$$\dot{L} \leq -\kappa_1 L - \kappa_2 L^l + d, \tag{71}$$

where $\kappa_1 = \min\Big\{\frac{\pi}{k_\star(t)}c_\star, \rho_\star, 2\widehat{\tau}_{\star 1}\Big\}, \kappa_2 = \min\Big\{\Big(\frac{\pi}{k_\star(t)}\Big)^l \mu_\star, 2^l\tau_{\star 2}, \frac{1}{1+l}(2\rho_\star)^l\Big\}$.

By virtue of Theorem 5.2 of [43], there always exists a finite time $\bar{t}$ such that $L \geq (2d/\kappa_2)^{(1/l)}$ for all $t \in [0, \bar{t}]$. Thus for all $t \in [0, \bar{t}]$, one has $\dot{L} \leq -\kappa_1 L - \kappa_2 L^l/2$, and it then comes from Lemma 3 that the fast finite-time stability of the closed-loop system can be ensured with a finite settling time $\overline{T} \leq \frac{1}{\kappa_1(1-l)} \ln\big((2\kappa_1 L^{1-l}(0) + \kappa_2)/\kappa_2\big)$. Furthermore, it is readily seen that $\bar{t} \leq \overline{T}$. Therefore, for $\forall t > \overline{T}$, $L \leq (2d/\kappa_2)^{(1/l)}$. Then all internal error signals will converge into the following compact sets

$$\begin{cases} z_\star \leq k_{b_\star}\sqrt{1-\exp\Big(-2\left(2d/\kappa_2\right)^{\frac{1}{l}}\Big)}, \\ z_\star \geq k_{a_\star}\sqrt{1-\exp\Big(-2\left(2d/\kappa_2\right)^{\frac{1}{l}}\Big)}, \\ |\tilde{\Xi}_V| \leq \sqrt{2\rho_V}\left(2d/\kappa_2\right)^{\frac{1}{l}}, |\tilde{\Xi}_\gamma| \leq \sqrt{2\rho_\gamma}\left(2d/\kappa_2\right)^{\frac{1}{l}}, \\ |\tilde{\Xi}_Q| \leq \sqrt{2\rho_Q}\left(2d/\kappa_2\right)^{\frac{1}{l}}, |\tilde{\Xi}_\alpha| \leq \sqrt{2\rho_\alpha}\left(2d/\kappa_2\right)^{\frac{1}{l}}, \\ |y_\gamma| \leq \sqrt{2}\Big(2d/\kappa_2\Big)^{\frac{1}{2l}}, |y_\alpha| \leq \sqrt{2}\Big(2d/\kappa_2\Big)^{\frac{1}{2l}}, \\ |y_Q| \leq \sqrt{2}\left(2d/\kappa_2\right)^{\frac{1}{l}}, \end{cases} \tag{72}$$

in finite time. Next, we prove that the constraints are never violated. From (62), (68) and (71), we note that all closed-loop signals are semi-globally-uniformly-ultimately-bounded and $\tan\Big(\frac{\pi z_\star^2}{2k_\star^2(t)}\Big) \in L_\infty$, then we conclude that $z_\star \in (k_{a_\star}, k_{b_\star})$ for $\forall t > 0$. This completes the proof. ■

REFERENCES

[1] C. Mu, Z. Ni, C. Sun, and H. He, "Air-breathing hypersonic vehicle tracking control based on adaptive dynamic programming," *IEEE Transactions on Neural Networks and Learning Systems,* vol. 28, no. 3, pp. 584-598, Mar. 2017.

[2] X. Bu, "Air-Breathing hypersonic vehicles funnel control using neural approximation of non-affine dynamics," *IEEE/ASME Transactions on Mechatronics,* vol. 23, no. 5, pp. 2099-2108, Oct. 2018.

[3] L. Wu, X. Yang, and F. Li, "Nonfragile output tracking control of hypersonic air-breathing vehicles with an LPV model," *IEEE/ASME Transactions on Mechatronics,* vol. 18, no. 4, pp. 1280-1288, Aug. 2013.

[4] J. Liu, H. An, Y. Gao, C. Wang, and L. Wu, "Adaptive control of hypersonic flight vehicles with limited angle-of-attack," *IEEE/ASME Transactions on Mechatronics,* vol. 23, no. 2, pp. 883-894, Apr. 2018.

[5] H. An, Q. Wu, C. Wang, and X. Cao, "Scramjet operation guaranteed longitudinal control of air-breathing hypersonic vehicles," *IEEE/ASME Transactions on Mechatronics,* DOI: 10.1109/TMECH.2020.2983521.

[6] R. Zuo, Y. Li, M. Lv, X. Wang, and Z. Liu, "Realization of trajectory precise tracking for hypersonic flight vehicles with prescribed performances," *Aerospace Science and Technology,* vol. 111, pp. 106554, Apr. 2021.

[7] X. Bu, Y. Xiao, and H. Lei, "An adaptive critic design-based fuzzy neural controller for hypersonic vehicles: predefined behavioral nonaffine control," *IEEE/ASME Transactions on Mechatronics,* vol. 24, no. 4, pp. 1871-1881, Aug. 2019.

[8] J. T. Parker, A. Serrani, S. Yurkovich, M. A. Bolender, and D. B. Doman, "Control-oriented modeling of an air-breathing hypersonic vehicle," *Journal of Guidance, Control, and Dynamics,* vol. 30, no. 3, pp. 856-869, May 2007.

[9] Z. Dong, Y. Li, M. Lv, and R. Zuo, "Adaptive accurate tracking control of HFVs in the presence of dead-zone and hysteresis input nonlinearities," *Chinese Journal of Aeronautics,* vol. 34, no. 5, pp. 642-651, Jan. 2021.

[10] H. Xu, M. Mirmirani, P. Ioannou, "Adaptive sliding mode control design for a hypersonic flight vehicle," *Journal of Guidance, Control, and Dynamics,* vol. 27, pp. 829-838, Sep. 2004.

[11] D. Preller, and M. Smart, "Longitudinal control strategy for hypersonic accelerating vehicles," *Journal of Spacecraft and Rockets,* vol. 52, no. 3, pp. 993-999, May 2015.

[12] Q. Wang, and R. Stengel, " Robust nonlinear control of a hypersonic aircraft," *Journal of Guidance, Control, and Dynamics,* vol. 23, no. 4, pp. 577-585, Jul. 2000.

[13] B. Xu, C. Yang, and Y. Pan, "Global neural dynamic surface tracking control of strict-feedback systems with application to hypersonic flight vehicle," *IEEE Transactions on Neural Networks and Learning Systems,* vol. 26, no. 10, pp. 2563-2575, Oct. 2015.

[14] X. Bu, X. Wu, F. Zhu, J. Huang, Z. Ma, and R. Zhang, "Novel prescribed performance neural control of a flexible air-breathing hypersonic vehicle with unknown initial errors," *ISA Transactions,* vol. 59, pp. 149-159, 2015.

[15] X. Hu, B. Xu, and C. Hu, "Robust adaptive fuzzy control for HFV with parameter uncertainty and unmodeled dynamics," *IEEE Transactions on Industrial Electronics,* vol. 65, no. 11, pp. 8851-8860, Nov. 2018.

[16] L. X. Wang, "Stable adaptive fuzzy control of nonlinear systems," *IEEE Transactions on Fuzzy Systems,* vol. 1, no. 2, pp. 146-155, May 1993.

[17] L. Dou, M. Du, Q. Mao, Q. Zong, "Finite-time nonsingular terminal sliding mode control-based fuzzy smooth-switching coordinate strategy for AHV-VGI," *Aerospace Science and Technology,* vol. 106, Nov. 2020.

[18] X. Zhang, Q. Zong, L. Dou, B. Tian, and W. Liu, "Improved finite-time command filtered backstepping fault-tolerant control for flexible hypersonic vehicle," *Journal of the Franklin Institute,* vol. 357, pp. 5485-5501, Mar. 2020.

[19] Y. Chen, Y. Wei, G. Duan, and L. Tan, "Robust finite time tracking control of flexible hypersonic vehicle with uncertainties," *2020 IEEE 4th Information Technology, Networking, Electronic and Automation Control Conference (ITNEC 2020).*

[20] H. Li, S. Zhao, W. He, and R. Lu, "Adaptive finite-time tracking control of full state constrained nonlinear systems with dead-zone," *Automatica,* vol. 88, no. 3, pp. 99-107, Jan. 2019.

[21] F. Wang, B. Chen, X. P. Liu, and C. Lin, "Finite-time adaptive fuzzy tracking control design for nonlinear systems," *IEEE Transactions on Fuzzy Systems,* vol. 26, no. 3, pp. 1207-1216, Jun. 2018.

[22] Y. Li, K. Li, and S. Tong, "Finite-time adaptive fuzzy output feedback dynamic surface control for MIMO nonstrict feedback systems," *IEEE Transactions on Fuzzy Systems,* vol. 27, no. 1, pp. 96-110, Jan. 2019.

[23] S. Sui, C. L. P. Chen, and S. Tong, "Fuzzy adaptive finite-time control design for nontriangular stochastic nonlinear systems," *IEEE Transactions on Fuzzy Systems,* vol. 27, no. 1, pp. 172-184, Jan. 2019.

[24] D. Swaroop, J. K. Hedrick, P. P. Yip, and J. C. Gerdes, "Dynamic surface control for a class of nonlinear systems," *IEEE Transactions on Automatic Control,* vol. 45, no. 10, pp. 1893-1899, Oct. 2000.

[25] L. Fiorentini, A. Serrani, M. A. Bolender, and D. B. Doman, "Nonlinear robust adaptive control of flexible air-breathing hypersonic vehicles," *Journal of Guidance, Control, and Dynamics,* vol. 32, no. 2, pp. 401-416, Mar. 2009.

[26] Z. Wilcox, W. MacKunis, S. Bhat, R. Lind, and W. Dixon, "Lyapunov-based exponential tracking control of a hypersonic aircraft with aerothermoelastic effects," *Journal of Guidance, Control, and Dynamics,* vol. 33, no. 4, pp. 1213-1224, Jul. 2010.

[27] K. P. Tee, S. S. Ge, and E. H. Tay, "Barrier Lyapunov Functions for the control of output-constrained nonlinear systems," *Automatica* vol. 45, pp. 918-927, Apr. 2009.

[28] B. Xu, Z. K. Shi, F. C. Sun, and W. He, "Barrier Lyapunov function based learning control of hypersonic flight vehicle with AOA constraint and actuator faults," *IEEE Transactions on Cybernetics,* vol. 49, no. 3, pp. 1047-1057, Mar. 2019.

[29] H. An, H. W. Xia, and C. H. Wang, "Barrier Lyapunov function-based adaptive control for hypersonic flight vehicles," *Nonlinear Dynamics,* vol. 88, pp. 1833-1853, Jan. 2017.

[30] X. Tang, D. Zhai, and X. Li, "Adaptive fault-tolerance control based finite-time backstepping for hypersonic flight vehicle with full state constrains," *Information Sciences,* vol. 507, pp. 53-66, Jan. 2020.

[31] M. A. Bolender, and D. B. Doman, "A non-linear model for the longitudinal dynamics of a hypersonic air-breathing vehicle," AIAA Paper 2005-6255, Aug. 2005.

[32] M. A. Bolender, and D. B. Doman, "Nonlinear longitudinal dynamical model of an air-breathing hypersonic vehicle," *Journal of Spacecraft and Rockets,* vol. 44, no. 2, pp. 374-387, Mar. 2007.
[33] X. Bu, X. Wu, J. Huang, and D. Wei, "Robust estimation-free prescribed performance back-stepping control of air-breathing hypersonic vehicles without affine models," *International Journal of Control,* vol. 89, no. 11, pp. 2185-2200, Mar. 2016.
[34] J. Ni, Z. Wu, L. Liu, and C. Liu, "Fixed-time adaptive neural network control for nonstrict-feedback nonlinear systems with deadzone and output constraint," *ISA Transactions,* vol. 97, pp. 458-473, 2019.
[35] H. Yang, and D. Ye, "Adaptive fixed-time bipartite tracking consensus control for unknown nonlinear multi-agent systems: An information classification mechanism," *Information Science,* vol. 459, pp. 238-254, 2018.
[36] S. Yu, X. Yu, B. Shirinzadeh, and Z. Man, "Continuous finite-time control for robotic manipulators with terminal sliding mode," *Automatica,* vol. 41, no. 11, pp. 1957-1964, Nov. 2005.
[37] G. H. Hardy, J. E. Littlewood, and G. Polya. *Inequalities.* Cambridge university press, 1952.
[38] B. Cui, Y. Xia, K. Liu, and G. Shen, "Finite-time tracking control for a class of uncertain strict-feedback nonlinear systems with state constraints: a smooth control approach," *IEEE Transactions on Neural Networks and Learning Systems,* DOI: 10.1109/TNNLS.2019.2959016.
[39] M. Lv, B. De Schutter, W. Yu, W. Zhang, and S. Baldi, "Nonlinear systems with uncertain periodically disturbed control gain functions: adaptive fuzzy control with invariance properties," *IEEE Transactions on Fuzzy Systems,* vol. 28, no. 4, pp. 746-757, Apr. 2020.
[40] M. Lv, S. Baldi, and Z. Liu, "The non-smoothness problem in disturbance observer design: A set-invariance-based adaptive fuzzy control method," *IEEE Transactions on Fuzzy Systems,* vol. 27, no. 3, pp. 598-604, Mar. 2019.
[41] M. Lv, W. Yu, and S. Baldi, "The set-invariance paradigm in fuzzy adaptive DSC design of large-scale nonlinear input-constrained systems," *IEEE Transactions on Systems, Man, and Cybernetics: Systems,* vol. 51, no. 2, pp. 1035-1045, Feb. 2021.
[42] B. Xu , Y. Shou, J. Luo, H. Pu , and Z. Shi, "Neural learning control of strict-feedback systems using disturbance observer," *IEEE Transactions on Neural Networks and Learning Systems,* vol. 30, no. 5, pp. 1269-1307, May 2019.
[43] S. P. Bhat and D. S. Bernstein, "Finite-time stability of continuous autonomous systems," *SIAM Journal on Control and Optimization,* vol. 38, no. 3, pp. 751-766, Feb. 2000.
[44] M. Lv, W. Yu, J. Cao, and S. Baldi, "Consensus in high-power multiagent systems with mixed unknown control directions via hybrid Nussbaum-based control," *IEEE Transactions on Cybernetics,* 2020, doi:10.1109/TCYB.2020.3028171.
[45] M. Lv, W. Yu, J. Cao, and S. Baldi, "A separation-based methodology to consensus tracking of switched high-order nonlinear multiagent systems," *IEEE Transactions on Neural Networks and Learning Systems,* 2021, doi:10.1109/TNNLS.2021.3070824.

Maolong Lv received the B.Sc. degree in Electrical Engineering and Automation, and M.Sc. degree in Control Science and Engineering from Air Force Engineering University, Xi'an, China, in 2014, and 2016 respectively. He is currently pursuing his Ph.D. degree in Systems and Control at the Delft Center for Systems and Control, Delft University of Technology, The Netherlands. His research interests include adaptive learning control, reinforcement learning, swarm control and switched systems with applications in multi-agent systems and unmanned and/or autonomous systems. Mr. Lv was awarded a Descartes Excellence Fellowship from the Institut Francais des Pays-Bas in 2018, which allowed him a research visit and a cooperation with the University of Grenoble on the topic of adaptive networked systems with emphasis on ring stability analysis for mixed traffic with human driven and autonomous vehicles from 2018 to 2019.

Yongming Li received the B.S. degree and the M.S. degree in Applied Mathematics from Liaoning University of Technology, Jinzhou, China, in 2004 and 2007, respectively. He received the Ph.D. degree in Transportation Information Engineering Control from Dalian Maritime University, Dalian, China in 2014. He is currently a Professor in the College of Science, Liaoning University of Technology. His current research interests include adaptive control, fuzzy control and neural networks control for nonlinear systems.

Wei Pan received the Ph.D. degree in Bioengineering from Imperial College London in 2016. He is currently an Assistant Professor at Department of Cognitive Robotics, Delft University of Technology. Until May 2018, he was a Project Leader at DJI, Shenzhen, China, responsible for machine learning research for DJI drones and AI accelerator. He is the recipient of Dorothy Hodgkins Postgraduate Awards, Microsoft Research Ph.D. Scholarship and Chinese Government Award for Outstanding Students Abroad, Shenzhen Peacock Plan Award. He is an active reviewer and committee member for many international journals and conferences. His research interests include machine learning and control theory with applications in robotics and aerospace.

Simone Baldi received the B.Sc. degree in electrical engineering, and the M.Sc. and Ph.D. degrees in automatic control systems engineering from the University of Florence, Italy, in 2005, 2007, and 2011, respectively. He is currently professor at the School of Mathematics, Southeast University, with a guest position at the Delft Center for Systems and Control, Delft University of Technology, where he was assistant professor. He was awarded outstanding reviewer of Applied Energy (2016), Automatica (2017), and IET Control Theory and Applications (2018). He is subject editor of International Journal of Adaptive Control and Signal Processing and an Associate Editor of IEEE Control Systems Letters. His research interests include adaptive and switched systems with applications in networked control and multi-agent systems.